CHARACTERIZATION OF GREENHOUSE GAS EMISSIONS FROM STORAGE OF WOODY BIOMASS: AN INCUBATION STUDY

By

Carisse Jianina Marie Barrios Geronimo

A Thesis Presented to

The Faculty of Humboldt State University

In Partial Fulfillment of the Requirements for the Degree

Master of Science in Environmental Systems: Energy, Technology and Policy

Committee Membership

Dr. Sintana Vergara, Committee Chair

Dr. Kevin Fingerman, Committee Member

Dr. Charles Chamberlin, Committee Member

Dr. Margaret Lang, Program Graduate Coordinator

December 2020

ABSTRACT

CHARACTERIZATION OF GREENHOUSE GAS EMISSIONS FROM STORAGE OF WOODY BIOMASS: AN INCUBATION STUDY

Carisse Geronimo

Biomass energy plays a small but significant role in the current renewable energy portfolio and is a promising alternative pathway for woody residues that would otherwise be considered waste. These woody residues are often stored in large piles prior to combustion, and greenhouse gas emissions from this storage phase of the bioenergy supply chain are uncertain and understudied. This incubation study investigates the effects of three environmental factors on emissions from decomposition of woody biomass stored in chip piles. Incubation experiments were conducted, subjecting chambers of *Sequoia sempervirens* woodchips to different levels of temperature, oxygen concentration, and moisture content, and measuring the resulting greenhouse gas emissions (CO_2, CH_4, N_2O) over thirty days. Notably, CH_4 was detected in concentrations above ambient levels, indicating that environmental conditions used in this study were conducive to anaerobic decomposition. Using a three-way repeated measures ANOVA, we found that temperature and moisture had significant effects on CO_2 emissions ($p < 0.005$ and $p < 0.001$, respectively). Oxygen and moisture had significant effects on CH_4 emissions ($p < 0.05$). No significant effects of these variables were detected for N_2O emissions. High temperature and high oxygen treatments were

found to be positively correlated with increased total CO_2 and CH_4 emissions. Understanding the key drivers of emissions from woody biomass can allow for better estimation of greenhouse gas emissions from the storage phase of the bioenergy supply chain.

ACKNOWLEDGEMENTS

It is with immense gratitude that I acknowledge the support of my committee chair, Dr. Sintana Vergara. I am thankful for her endless encouragement and for inspiring me long before I arrived at Humboldt State University. I will forever be motivated by her passion, brilliance, and kindness. I want to thank Dr. Kevin Fingerman for his skillful guidance and feedback throughout the entire course of this study. He has also been a wonderful professor and supportive mentor. Finally, I owe my deepest appreciation to Dr. Charles Chamberlin for his patient and thoughtful approach to making suggestions for the study and especially in writing this thesis. Working with this thesis committee has been a dream come true.

I extend my heartfelt thanks to Andrea and Don Tuttle for establishing their fellowship for clean energy studies. Words cannot express the gratitude I have felt for this financial support and the opportunities it has granted me. I also thank Andrea for being the most motivational mentor in multiple ways: as a fabulous lecturer in the Climate Change and Land Use course, as a role model involved with climate and forestry policy, and as a dear friend.

This study received generous funding from the California State University Agricultural Research Institute. Match funding was provided by the California Energy Commission through the California Biopower Impacts Project. Without this support, this project would not have been possible.

I would like to thank the team at the Schatz Energy Research Center for inspiring me and introducing me to the world of renewable energy work. I would especially like to thank Arne Jacobson for his warm encouragement and guidance, Mark Severy for being a terrific project manager, and Cassidy Barrientos, Liszet Burgueño, and Karly Johnson for their invaluable contributions during different phases of this incubation study.

To my friends from the ETaP program (Alex Ross, Amin Younes, Anamika Singh, Chih-Wei Hsu, Grishma Raj Dahal, Julie Anderson, Nicole Salas, Thomas Tu): I am grateful for getting to know each of you and for our solidarity around the mysterious workings of being a grad student. Thank you, Grishma and Alex, for all the laughs over dozens of tacos, burritos, and the occasional glass of orange juice.

Without support from many other friends, I could not have persevered through this process. I owe my heartfelt thanks to: Emma Cody and Anna Machado for making me feel at home in Humboldt, Amanda Masse and Michelle Aldrete for rock climbing and backpacking with me, David Kwasman for being my sounding board on everything from baked goods to navigating adulthood, Jay Joshi for motivating, annoying, and making me laugh, Hannah Nguyen for guiding me and showing me loving-kindness, and Michael Perez for never letting me go hungry and always believing in me.

Lastly, I am thankful for my brother, Miah, and my sister and best friend, Chelsea, who inspire me to be the best version of myself. I am forever indebted to my parents, Jason and Claudette, who have given up so much to give me access to the opportunities and experiences that are making me who I am. I dedicate this work to them.

TABLE OF CONTENTS

LIST OF TABLES

LIST OF FIGURES

LIST OF APPENDICES

CHAPTER 1. INTRODUCTION

1.1 Background

1.1.1 Biomass Energy in California

The Renewable Portfolio Standards (RPS) program in the United States recognizes biomass energy as an eligible source of renewable energy (Barbose, 2018). The California Energy Commission (CEC) reports that approximately 3% of the state's total power came from biomass energy in 2018 (CEC, 2019). This accounted for roughly 10% of California's renewable energy generation (CEC, 2019). This project aims to investigate an uncertain and understudied portion of the bioenergy supply chain. Emissions from storage of biomass feedstock are often overlooked and may play a large role in the overall carbon flux of biomass utilization (Lottes, 2014; Sahoo et al., 2018).

Combustion of biomass residue also serves as a way to dispose of residues from agricultural and forestry sectors (Mayhead and Tittman, 2012). While the amount of biomass available for harvesting varies over time due to changes in climate and forest management, the state of California alone has been reported to produce up to 30 million tons (wet weight) of biomass feedstock annually (Jenkins et al., 2009). Energy production from biomass is generally seen as a promising utilization pathway for this abundance of feedstock, but questions remain regarding its renewability, associated costs and benefits, as well as the net carbon flux of biomass combustion for energy (Jenkins et al.,

2009). Electricity production from biomass is a promising alternative for woody residue that would otherwise be considered waste (Pecenka et al., 2018).

1.1.2 Storage of Woody Biomass

Biomass in the form of woodchips and wood pellets is the most common feedstock for power plants and biorefineries (Mobini et al., 2014). Indoor storage of chips (in silos or other enclosed permanent structures) is not typical due to the high cost of the required infrastructure (Noll and Jirjis, 2012, Sahoo et al., 2018). Outdoor storage is favorable due to flexibility of storage location as well as relatively low associated capital costs (Sahoo et al., 2018). This method, however, may cause increases in overall cost; exposure to moisture from precipitation and the surrounding environment facilitates relatively high dry matter loss and reduced feedstock energy content due to decomposition of the organic matter, decreasing the efficiency and profitability of bioenergy (He et al., 2014; Sahoo et al., 2018). Moreover, percent DML has been reported as positively related to total gas emissions (He et al., Whittaker et al., 2016).

Greenhouse gas emissions from this decomposition process, especially in the context of biomass supply chains, is currently understudied (Jamsen et al., 2015; Sahoo et al., 2018). These emissions may have significant impacts on the net climate footprint of bioenergy. Additionally, several fatalities and several more injuries have been reported in relation to the atmosphere created by depletion of oxygen and the simultaneous creation of carbon monoxide, carbon dioxide, methane, and other volatile organic compounds (VOCs) during woody biomass storage, particularly in poorly ventilated spaces including

storage structures and cargo vessels (Meier et al., 2016; Svedberg et al., 2004). A better understanding of the storage phase of the bioenergy process would inform the feasibility and climate impacts of this technology and allow for meaningful contributions to future life cycle assessments (Noll and Jirjis, 2012; Kuang et al., 2008).

1.1.3 Biomass Decomposition

Biomass storage piles, which may remain undisturbed for months at a time, are naturally subject to biological decomposition (He et al., 2011). The microbial activity associated with this decomposition leads to increased temperature, diminished energy content, and gas formation (Noll and Jirjis, 2012). Sub-optimal storage conditions may accelerate rates of decomposition, resulting in serious consequences such as 1) spontaneous combustion due to extreme increases in temperature, 2) diminished economic viability due to energy content loss, as well as 3) significant health and environmental impacts due to the production of greenhouse gases (Sahoo et al., 2018; Kuang et al., 2008; Meier et al., 2016).

This study is motivated by the potential for mitigating these effects, most especially in relation to investigating the understudied off-gassing of stored woody biomass. A variety of conclusions have been drawn from recent studies about greenhouse gas emissions from storage of woody residue; this may be carbon neutral, or be a net source or net sink of emissions (Covey and Megonigal, 2018; Alakoski et al., 2016). This variability is partially dependent on a set of environmental factors and conditions regarding biomass and its storage. The most influential of these are temperature, oxygen

concentration, and humidity or moisture content (Kuang et al., 2009; Meier et al., 2016). Other factors include chip particle size, tree species of feedstock supply, storage pile geometry and size, time of storage, ventilation, geographical location, and precipitation rates (Noll and Jirjis, 2012; Sahoo et al., 2018).

1.1.4 Factors Affecting Decomposition

The following three sections summarize relevant findings from the available literature regarding the major factors of pile temperature, oxygen concentration, and moisture content.

1.1.4.1 Temperature

The temperature of piled feedstock is known to vary spatially and temporally (Pecenka et al., 2018). Temperature phases of decomposition are dependent on the composition of the biomass that is available for microorganisms to break down (Bedane et al., 2011). This biological activity occurs at relatively high rates when the feedstock is new and nutrient-rich (He et al., 2014). The effect of this activity is generally observed most clearly in the first several weeks of storage, and slowly declines over time (Jamsen et al., 2015). The general trend which describes the decomposition of biodegradable material includes a mesophilic phase (which is characterized by steady warming of the material up to approximately 40°C), a thermophilic phase (which entails a short and intense burst of microbial activity during which the temperature may spike to approximately 65°C), and a maturation phase (which is characterized by gradual decrease

in the temperature of the material, indicating decreased microbial activity) (Jamsen et al., 2015; Noll and Jirjis, 2012).

The temperature within piles also varies spatially (Bedane et al., 2011). Biomass near the surface of the pile tends to remain close to ambient temperature, while the core of the pile reaches the highest temperatures during storage (Bedane et al., 2011). The column-shaped portion directly above the central core is relatively warm as well, as a result of convection (which causes the generated heat to rise) and insulation (due to shielding by the surrounding chips or pellets in the pile) (Andersen et al., 2010). Gases are drawn in from the sides of the pile towards the core and a great majority of gas emissions (>85%) are vented through the top center portion of the pile (Andersen et al., 2010; Jamsen et al., 2015). This “chimney effect” (Figure 1) has been reported in several studies involving biomass piles and related structures such as compost windrows and manure stockpiles (Andersen et al., 2010; Sommer et al., 2004).

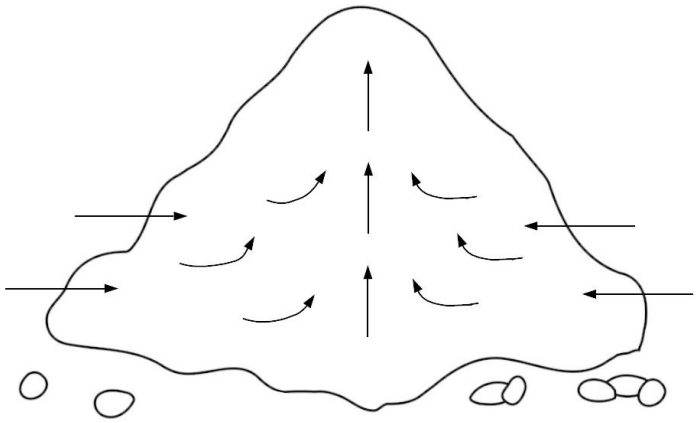

Figure 1. Conceptual drawing of the "chimney effect" observed in piles of biodegradable material (adapted from Andersen et al., 2010.), showing gas drawn in from the sides of the pile and being emitted through the top center section of the pile

Additionally, extreme temperature increases within storage piles have been reported to cause spontaneous ignition, which decreases the potential electricity generation of bioenergy technology, poses a health risk for plant operators and the local community, and creates high-cost management and property issues (Alakoski et al., 2015; Jirjis and Theander, 2008). The risk of fire is increased as storage pile size increases (Jamsen et al., 2015). Improvements to storage conditions as they relate to temperature have environmental consequences as well as implications for human health and safety.

1.1.4.2 Oxygen Concentration

The availability of oxygen is also a major factor affecting greenhouse gas emissions from biological decomposition (Kuang et al., 2008). Oxygen is consumed in chemical reactions that occur during decomposition, resulting in oxygen depletion and generation of products such as CO_2 and CO (Kuang et al., 2008). In a sealed container, or a poorly-ventilated space that does not allow for oxygen replacement, this oxygen depletion eventually leads to the creation of anaerobic conditions (Andersen et al., 2010).

In these anaerobic conditions, methane can be produced by microorganisms (Whittaker et al., 2016; Alakoski et al., 2015). Biomass storage piles, which are generally created to last extended periods of time to maintain availability of bioenergy feedstock, are often left undisturbed for months at a time (Whittaker et al., 2016; Sahoo et al., 2018). When stored feedstock is not turned or otherwise aerated, anaerobic conditions may develop in “pockets” within storage piles, generating methane and related gaseous products (Sahoo et al., 2018). The extent to which methane is produced is a large source

of uncertainty in net GHG flux calculations for the life cycle of biomass energy, given that methane is a potent greenhouse gas (Lottes, 2014). Oxygen concentrations are linked to the "chimney effect" (Figure 1) as well (Andersen et al., 2010). Spatial variation of oxygen concentration within a pile or windrow follows the inverse of the trend observed with temperature in this regard; oxygen concentrations are lowest in the core region, greatest among the outer regions, and moderate in the center column (Andersen et al., 2010).

1.1.4.3 Moisture Content

Moisture content is also known to impact microbial decomposition (Bedane et al., 2011; Jamsen et al., 2015). The range of moisture content for harvested woodchips is approximately 40-60%, with a typical value of 50% (Whittaker et al., 2016). Pile storage of these woodchips results in moisture redistribution, with the exposed regions of the pile becoming relatively wet and the inner regions becoming relatively dry (Noll and Jirjis, 2012).

Decreased heating value of the woody biomass as a result of dry matter loss is especially prominent in the case of high-moisture woodchip storage (Sahoo et al., 2018). For biomass with an initial moisture content of 55%, the average dry matter loss was observed to range from 0.7%-1.5% per month (Afzal et al., 2010; Thornqvist, 1985; Bedane, 2011). To slow down the decomposition process, drying of forest chips to 20-30% moisture content (wet basis) followed by tarping is recommended (Jamsen et al.,

2015; Pecenka et al., 2018). Better management of this moisture content can improve cost-efficiency of the bioenergy supply chain (Anerud et al., 2019).

The available moisture also influences the viability and potential activity of microbes that inhabit the wood chips which influences the gas production that is possible as a result of microbial metabolism (Alakoski et al., 2015). Moisture within a biomass storage pile affects the overall porosity of the pile and therefore the flow of gas within it (Jamsen et al., 2015). In this way, the moisture content is strongly tied to metabolic activity, and may impact the rates at which products such as CH_4 and N_2O are generated (Jamsen et al., 2015).

1.2 Thesis Objectives

The main objectives of this study include 1) observing the effects of key environmental factors (temperature, oxygen, moisture) on greenhouse gas emissions (carbon dioxide, methane, and nitrous oxide) from storage of woody biomass, 2) measuring the cumulative greenhouse gas emissions from this incubation study, and 3) generating a predictive model for these greenhouse gas emissions. These have been prioritized to inform best management practices for minimizing energy content loss, reducing greenhouse gas emissions, and mitigating risk of fire during long-term periods of biomass storage.

CHAPTER 2. METHODS

In this study, locally sourced wood chips were exposed over time to a variety of environmental conditions which simulate conditions likely to be found in chip piles. This study aimed to facilitate a relatively high level of control of these environmental factors within chambers that act as microcosms of biomass piles.

The three major variables influencing decomposition rates of biomass -- temperature, oxygen concentration, and moisture content (Kuang et al., 2009) -- were manipulated in the laboratory experiments, and concentrations of resulting greenhouse gases were measured over the duration of the experiment. Several incubation studies of similar scope (He et al., 2011; Pier and Kelly, 1997; Chen et al., 2000) were explored in order to choose an appropriate length of incubation for this study. The selected incubation duration (30-31 days) was determined as a result of this literature review.

The set of incubation treatments are outlined in a 3 x 3 x 2 experimental matrix. The study undertook three rounds of experiments, using one temperature treatment at a time, with six treatments given concurrently per round of incubation, and three replicates per treatment. Three oxygen concentration treatments (0%, 10%, and 20%) and two biomass moisture content levels (50% and 70%, wet basis) were used for each of the three incubation temperatures (20°C, 40°C, and 60°C) (Table 1).

2.1 Incubation Study Concept

For each of the three environmental factors (temperature, oxygen concentration, and moisture content), a range of values was observed in piles at an active biomass power plant in the northwestern region of the United States (additional information on these values is found in Appendix A). A review of available literature was performed to collect information regarding the variation of temperature, oxygen concentration, and moisture in biomass incubation studies. The field observations in combination with values from literature were used to inform the matrix of environmental conditions that comprised the treatments for this study.

The levels within these environmental factors were expected to yield some differences on biological decomposition and therefore rates of gas production, mainly due to the impact of these factors on the metabolic activity of microbes (Alakoski et al., 2016; He et al., 2014). Although a number of studies have used a combination of these variables (in addition to others), the experimental matrix of 3 x 3 x 2 (temperature, oxygen concentration, and moisture content) described herein has not yet been reported for use in a biomass incubation study.

Each incubation treatment (a unique combination of levels within the three environmental variables) represents conditions from different regions of a biomass pile over time. Lower oxygen concentrations and lower moisture content levels are representative of regions closer to the core, while higher oxygen concentrations and higher moisture content levels are representative of the outer regions of a pile.

Temperature within a pile is largely variable over time but also varies spatially, with higher temperatures observed in the core as well (as discussed in 1.1.4.1 Temperature).

Table 1. Outline of treatments for incubation study, performed once for each of the three temperature levels (20°C, 40°C, and 60°C).

Chamber	Oxygen Treatment	Moisture Content
1	0%	50%
2	0%	50%
3	0%	50%
4	0%	70%
5	0%	70%
6	0%	70%
7	10%	50%
8	10%	50%
9	10%	50%
10	10%	70%
11	10%	70%
12	10%	70%
13	20%	50%
14	20%	50%
15	20%	50%
16	20%	70%
17	20%	70%
18	20%	70%

2.2 Incubation Setup

Samples of biomass chips were incubated in custom-built chambers for each phase of this incubation study. The biomass chips were tested for moisture content and prepared for either 50% or 70% moisture (wet basis). Each chamber cavity was flushed with a gas mixture corresponding to 0%, 10%, or 20% O_2. The chambers were placed into a laboratory oven for the duration of the incubation period. Gas samples were extracted every two to three days and analyzed for concentrations of oxygen, carbon dioxide, methane, and nitrous oxide. Gas replacement was performed following gas sample extraction to keep the gas volume consistent and to return oxygen concentrations to initial levels in each of the chambers.

2.2.1. Incubation Chamber Design

A customized incubation chamber design was developed for this experiment. Glass canning jars (Ball jars of approximately 0.949 L) were fitted with custom inlet and outlet ports consisting of on/off gas valves, barbs, barb adapters, O-rings, and PVC tubing. These ports were installed through circular holes (1/4” diameter) in metal jar lids. A schematic of the chamber design is shown in **Error! Reference source not found.**, and a picture is included in

Appendix B.

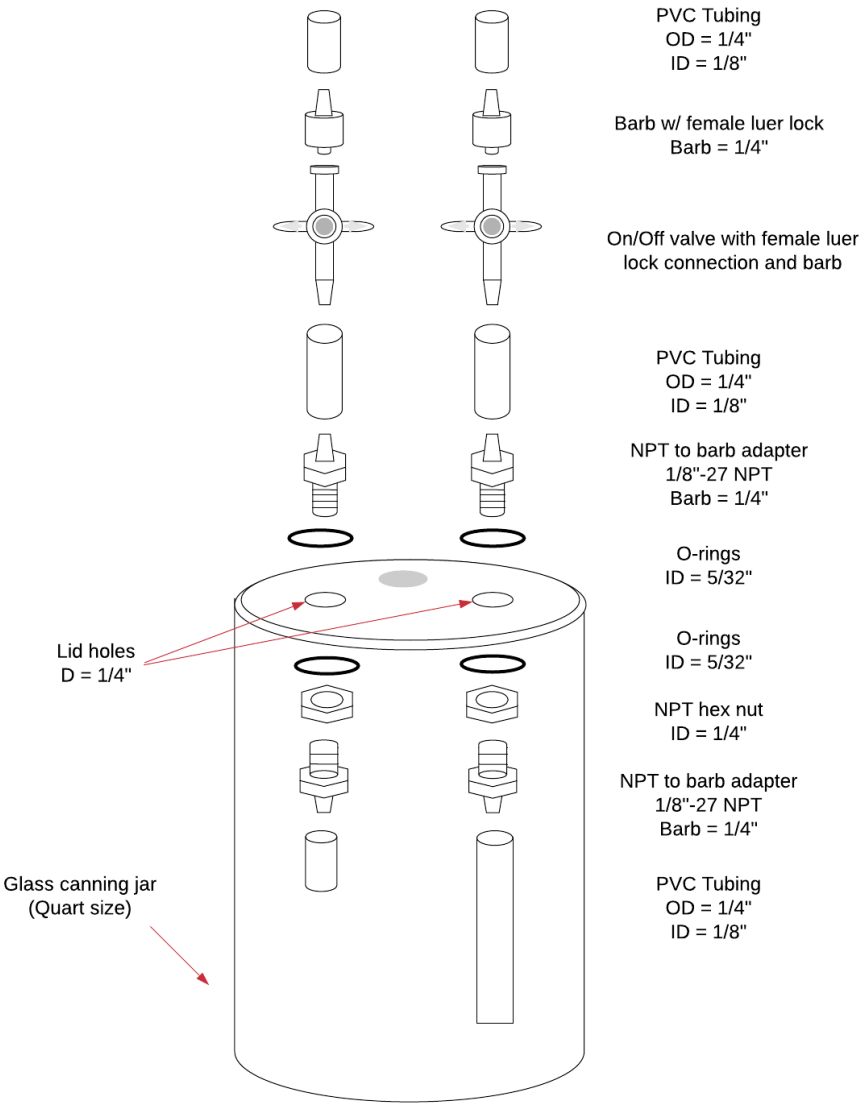

Figure 2. Schematic of incubation chamber design, displaying parts used for custom-built inlets and outlets for gas injection and extraction

The inlet and outlet ports were designed with different lengths of PVC tubing inside the chamber for increased efficiency in gas mixing. The inlet port had tubing that

reached the chamber bottom to facilitate the mixing of replacement gases throughout the chip sample. The outlet port had short tubing that allowed for unobstructed access to the mixed gases in the chamber headspace following manual chamber shaking (see 2.4.1 and 2.4.2 for additional details regarding use of ports during gas sampling).

The chamber design initially included a gas sample bag attachment on the outlet port to allow for the volume of the system to expand and maintain atmospheric pressure. This component was later deemed unnecessary due to the results of a chamber incubation test run (100 g of biomass in each chamber at 60°C for 28 days). The calculated change in pressure was 0.131 atm, which was considered negligible for purposes of this study.

2.2.2. Instruments for Gas Analysis

Two instruments were used in tandem to measure concentrations of relevant gases in the incubation chambers: a Picarro G2508 Gas Concentration Analyzer (Santa Clara CA, USA), to measure the concentrations of greenhouse gases and an Inficon 1,2-Channel 3000 Micro GC Gas Analyzer (Bad Ragaz, Switzerland), to measure the oxygen concentration.

2.2.2.1. Picarro GHG Analyzer

A Picarro G2508 cavity ringdown spectrometer (hereafter referred to as “GHG analyzer”) was used to analyze greenhouse gas concentrations for this study. This instrument has the capacity to measure five gases continuously and simultaneously

(carbon dioxide, methane, ammonia, nitrous oxide, and water vapor). An accessory pump (Picarro Closed System Pump A0702) was used to pull gaseous samples through the cavity of the GHG analyzer. A PVC plastic tube was installed at the outlet of the GHG analyzer to allow gases to escape the laboratory environment and vent into the air.

Calibration of the GHG analyzer was performed as outlined in the instrument manual provided by the manufacturer ("Picarro G2308/G2508 Analyzer for N_2O, NH_3, H_2O, CH_4, and CO_2 User's Manual"). It was calibrated to measure carbon dioxide, methane, and nitrous oxide using gas mixtures from Gasco Precision Calibration Mixtures (Oldsmar, Florida). Three calibration standards of differing concentrations were introduced to the GHG analyzer for each of the three aforementioned gases. The concentrations of calibration gases used were 725 ppm, 2000 ppm, and 11% CO_2; 5 ppm, 10 ppm, and 15 ppm CH_4; and 10 ppm, 50 ppm, 400 ppm N_2O. These values were selected based on ranges from results in published studies. The analyzer's reported concentration values and the gas standards' concentration values were plotted on the horizontal and vertical axes, respectively.

A linear best-fit equation was then calculated from the data for each gas. The slope and intercept of these equations were the "calibration values" that were inputted into the analyzer software under the "User Calibration" tab in the settings menu. These equations and their associated calibration data are shown in

Appendix C. This calibration process is outlined in the Picarro G2308/2508 Gas Concentration Analyzer User's Manual.

2.2.2.2. Cerity QA/QC & Gas Chromatograph

Oxygen concentrations were measured using an Inficon 1,2-Channel 3000 Micro GC Gas Analyzer (hereinafter referred to as "Micro GC"). This instrument contains two independent micro gas chromatograph channels, each with their own sample injector, detector, and high-resolution capillary column. The carrier gases required for use of this instrument (argon and helium), were filtered by Restek Super Clean Carrier Gas Filters. A PVC plastic tube was installed at the outlet of the Micro GC to allow gases to escape the laboratory environment and vent into the air.

Calibration of the Micro GC was performed according to the instrument manual provided by the manufacturer ("Inficon Micro GC 3000 Gas Analyzer Operating Manual"). The CO_2 calibration gas standards (described in Section 2.1.2.1) were introduced to the GC (gas chromatograph) inlet. The response curves from the GC were used to find a conversion factor to translate peak curve areas into concentration values.

2.2.3. Environmental Control

The apparatus needed for controlling the temperature and the gas concentrations of the incubation chambers are described in the following section. Moisture content control was not implemented due to negligible changes in moisture from gas sampling events throughout the study.

2.2.3.1. Laboratory Oven

The laboratory oven (Fisher Scientific Isotemp Oven) was set to a consistent temperature for the thirty-day duration of each incubation round (20°C, 40°C, or 60°C respectively). A PVC plastic tube was installed at the outlet port of the oven to allow gases to escape the laboratory environment and vent into the air.

This oven housed all eighteen chambers for each round of incubation. The chamber arrangement for the study is illustrated in **Error! Reference source not found.**. Because the oven was relatively small (approximately 2' by 3') and was set to a constant temperature for extended periods of time, the temperature was assumed to be uniform within the oven throughout the incubation experiments.

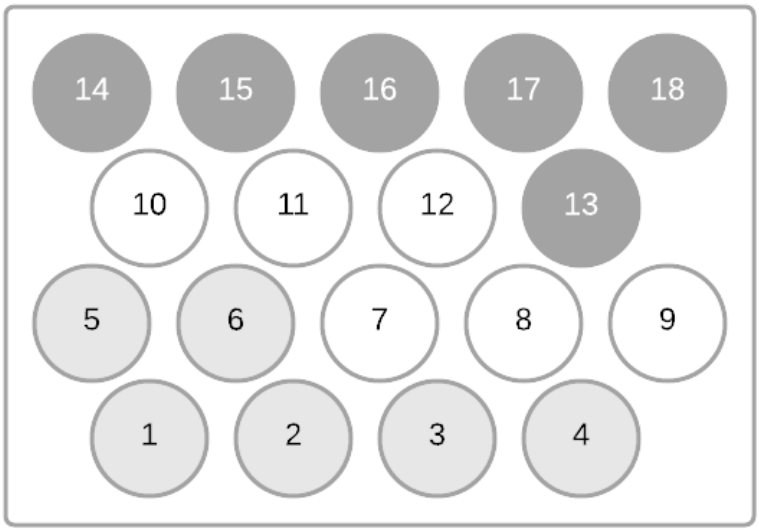

Figure 3. Overhead diagram of incubation chamber arrangement in oven with shading differences to denote oxygen concentration treatments

2.2.3.2. Gas Manifold

A custom gas manifold was assembled for the purpose of accurately mixing nitrogen and oxygen gas for chamber flushing. The schematic (Figure 4) displays the layout used for this study (and a picture is included in

Appendix B). One cylinder of 100% nitrogen (220 scf) and one cylinder of 100% oxygen (220 scf) were connected to gas regulators via flexible stainless-steel tubing. These tubes met at a junction in the manifold directly upstream of an on/off gas valve built in to allow gas to fill the manifold and related parts. Two WIKA gauges (Lawrenceville, GA) were downstream of this inlet valve, directly across from another on/off valve that led to the fittings for the lecture bottles. One gauge measured pressure from 0 to 600 psig (in increments of 2 psig) and the other gauge measured pressure from -30 to 0 psig. The main tubing then turned upwards to a vent valve oriented towards the fume hood.

The gas manifold allowed for flushing of the lecture bottle system with 100% N_2 to them for carrying the gas mixtures required for the incubation study. Preparing the mixtures for the 10% and 20% O_2 treatments in this study entailed supplying pressure in the gas manifold system to a calculated pressure with 100% O_2, shutting off the flow of the O_2, and pressurizing the system with 100% N_2 gas. Simply filling the lecture bottles with 100% N_2 created the gas required for the 0% O_2 treatment. The specific protocols used in creating the gas mixtures for all three oxygen treatments are outlined in 2.4.3.1 Gas Mixture Preparation/Lecture Bottle Filling.

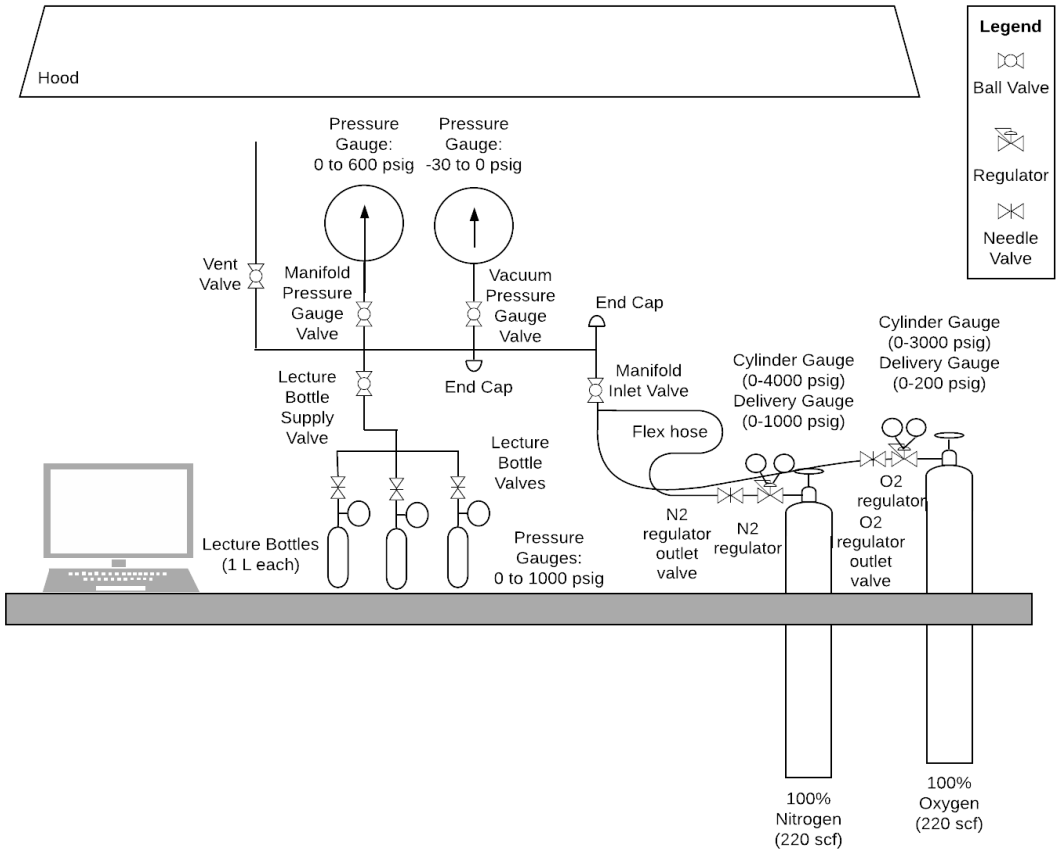

Figure 4. Plumbing and instrumentation diagram of gas manifold and mixing system (not to scale)

2.2.4. Additional Incubation Study Materials

For this incubation study, 50 mL and 10 mL Fisher Scientific Air-Tite™ All-Plastic Norm-Ject syringes were used for extraction and injection of gases during gas sampling events. Tedlar 0.5-liter sample bags with single polypropylene septum fittings from SKC, Inc. were used to deliver gas samples to the Micro GC. A Trossen Robotics 12V vacuum pump was used to empty contents of gas sample bags in between samples and to create negative pressure to pull gas through the incubation chambers during chamber flushing.

2.3. Sample Material

The sample material used for this study was composed of wood chips of the species *Sequoia sempervirens* (Coast redwood). These chips were obtained from a local landscape materials company that sourced the wood from Humboldt Redwood Company, LLC (HRC). HRC operations are certified to the standards of the Forest Stewardship Council. This feedstock was transported to the laboratory approximately 3 weeks after harvesting. Woodchip size was variable (picture in

Appendix B) and the material was a mix of bark and wood.

Approximately 150 g and 175 g of the sample material were added to the chambers assigned to 50% and 70% moisture, respectively. The average initial moisture content of the feedstock was measured to be 50%, and a custom protocol (2.4.1.2 Moisture Content Adjustment) was created to obtain the 70% moisture required for the additional treatments. This mass difference facilitated a consistent chamber headspace across moisture treatments.

2.4. Treatment Parameters

The following sections outline the procedures required for setting up each of the three environmental variables that were used in this study: moisture content, temperature, and oxygen concentration.

2.4.1. Moisture Content of Sample Material

Two moisture treatments were used in this incubation study. Wood chip material was brought to one of two moisture levels-- 50% or 70% (wet basis) for each of the three rounds of incubation.

2.4.1.1. Moisture Content Testing

Approximately 60 L of wood chips from the species *Sequoia sempervirens* were obtained, mixed thoroughly for representative sampling, and stored in airtight containers.

The following procedure for calculating moisture content was adapted from the "Standard Test Method for Moisture Analysis of Particulate Wood Fuels" by the American Society for Testing and Materials (ASTM) International (ASTM, 2006).

The laboratory oven was set to 104 °C. All masses were measured using a My Weigh iBalance 5500 scale and the readings were recorded to the nearest 0.01 g. The mass of four aluminum baking trays were recorded as "Tare Weight". A minimum of 50 g of wood chips was placed in each aluminum tray. The combined mass of the chips and tray was recorded as "Gross Wet Weight".

The trays were placed in the laboratory oven after reaching 104 °C. The trays of wood chips were left in the oven for at least 24 hours. The mass of each tray of chips was measured and recorded as "Gross Weight at 24H". The trays were returned to the oven and then masses were measured again after one hour, recorded as "Gross Weight at 25H". The total mass change (in percent) was calculated as the difference between Gross Weight at 24H and Gross Weight at 25H. If the change was less than or equal to 0.2%, the chips were removed and stored in airtight containers. If the change was greater than 0.2%, the chips were returned to the oven for additional drying. Once the mass change requirement was met, the final mass of each tray was recorded as "Final Gross Weight". The moisture content (wet basis) was then calculated using the equation below (moisture content (wet basis) $= \frac{w_i - w_f}{w_i - w_c}$

Equation 1

).

$$\text{moisture content (wet basis)} = \frac{w_i - w_f}{w_i - w_c}$$

Equation 1

where:

w_i = gross wet weight = initial weight of the chips and tray (g)

w_f = final gross weight = final weight of the chips and tray (g)

w_c = tare weight = tray weight (g)

2.4.1.2 Moisture Content Adjustment

Before beginning each round of incubation, the moisture content of the biomass sample was tested. If the moisture content of the biomass sample was below the designated moisture content treatment (50% or 70%), a calculated amount of water was distributed evenly to the feedstock to achieve the desired moisture content. This was done on a wet basis of moisture content by mass. Chip masses for each chamber are recorded in Appendix D.

2.4.2. Incubation Temperature

Each round of incubation occurred at a constant temperature. The incubation chambers were subjected to temperatures of 60 °C, 40 °C, and 20 °C in the laboratory oven for the first, second, and third rounds of incubation, respectively.

2.4.3. Oxygen Level in Incubation Chambers

Wood chips were stored in chambers with one of three oxygen concentrations for the study. This section outlines the procedure through which the gas manifold and gas mixing system (section 2.1.3.2) were used to create gas mixtures using pure nitrogen gas and oxygen gas. There are three gas mixture proportions of nitrogen and oxygen that were needed in order to treat the incubation chambers with the three selected oxygen concentrations; nitrogen to oxygen ratios of 8:2, 9:1 and 10:0 were needed for the 20%, 10%, and 0% oxygen treatments, respectively. The procedures in the following sections reference parts of the gas manifold that are shown in Figure 4.

2.4.3.1 Gas Mixture Preparation/Lecture Bottle Filling

The gas mixtures for this study were created in the laboratory using the custom gas manifold and associated gas mixing setup (section 2.1.3.2). This procedure was formulated with a final pressure target of 400 psig for each filled 1 L lecture bottle. Each lecture bottle contained enough pressure to flush approximately three incubation chambers with eight to nine times the chamber volume. The ratios of 8:2, 9:1 and 1:0 nitrogen gas to oxygen gas correspond to the 20%, 10%, and 0% oxygen treatments, respectively.

2.4.3.1.1 Mixing gas for the 20% O_2 treatment

A cylinder of 100% O_2 gas was used to supply enough pressure in the gas manifold system for the manifold pressure gauge to read 71 psig (visually approximated

between the gauge graduations of 70 and 72 psig). The manifold was left undisturbed for 3 minutes to allow internal pressure and temperature to stabilize. The lecture bottle valves were closed once the appropriate pressure was achieved, then the O_2 gas flow was shut off. The gas manifold was subsequently flushed with 100% N_2 gas for at least 3 seconds. The entire system was then pressurized to 100 psig with N_2 gas. The lecture bottle valves were opened to allow the gas to enter and mix while the delivery pressure of the N_2 gas was increased until the manifold pressure gauge read 400 psig. The lecture bottles were closed, and the gas flow was shut off once the appropriate pressure was achieved. Assuming all measurements are done as described above, this procedure yields a mixture of 20.7% O_2 and 79.3% N_2. Increased accuracy could be achieved using pressure gauges with more precise graduations.

2.4.3.1.2 Mixing gas for the 10% O_2 treatment

A cylinder of 100% O_2 gas was used to supply enough pressure in the gas manifold system for the manifold pressure gauge to read 28 psig. The manifold was left undisturbed for 3 minutes to allow internal pressure and temperature to stabilize. The lecture bottle valves were closed once the appropriate pressure was achieved, then the O_2 gas flow was shut off. The gas manifold was subsequently flushed with 100% N_2 gas for at least 3 seconds. The entire system was then pressurized to 100 psig with N_2 gas. The lecture bottle valves were opened to allow the gas to enter and mix while the delivery pressure of the N_2 gas was increased until the manifold pressure gauge read 400 psig. The lecture bottles were closed, and the gas flow was shut off once the appropriate pressure

was achieved. Assuming all measurements are done as described above, this procedure yields a mixture of 10.3% O_2 and 89.7% N_2. Increased accuracy could be achieved using pressure gauges with more precise graduations.

2.4.3.1.3 Filling lecture bottles with nitrogen (for the 0% O_2 treatment)

A cylinder of 100% N_2 was used to fill the lecture bottles to a pressure of 400 psig. The lecture bottle valves were closed once the appropriate pressure was achieved, then the N_2 gas flow was shut off and residual gas in the manifold was vented to the fume hood.

2.4.3.2. Gas Sample Bag Filling

Tedlar 10-liter sample bags with single polypropylene septum fittings from SKC, Inc. were filled with gas mixtures in preparation for incubation chamber flushing. Each gas sample bag included a polypropylene fitting that served as a hose/valve fitting and housed an injection septum. A pair of regulators in series were used to facilitate a low-pressure delivery of the gas mixtures from the lecture bottles to the gas sample bags. The gases in the lecture bottles were at a maximum of 400 psig and the delivery pressure to the gas sample bags was lowered to 30 psig using a series of regulators.

2.4.3.3. Incubation Chamber Flushing

Following gas mixture transfer to the 10 L sample bags, the setup in Figure 5 was used to flush the incubation chambers. Each sample bag was filled to approximately 90%

capacity (the maximum capacity recommended by the manufacturer). Each sample bag was used to flush one incubation chamber with eight to nine times the chamber volume.

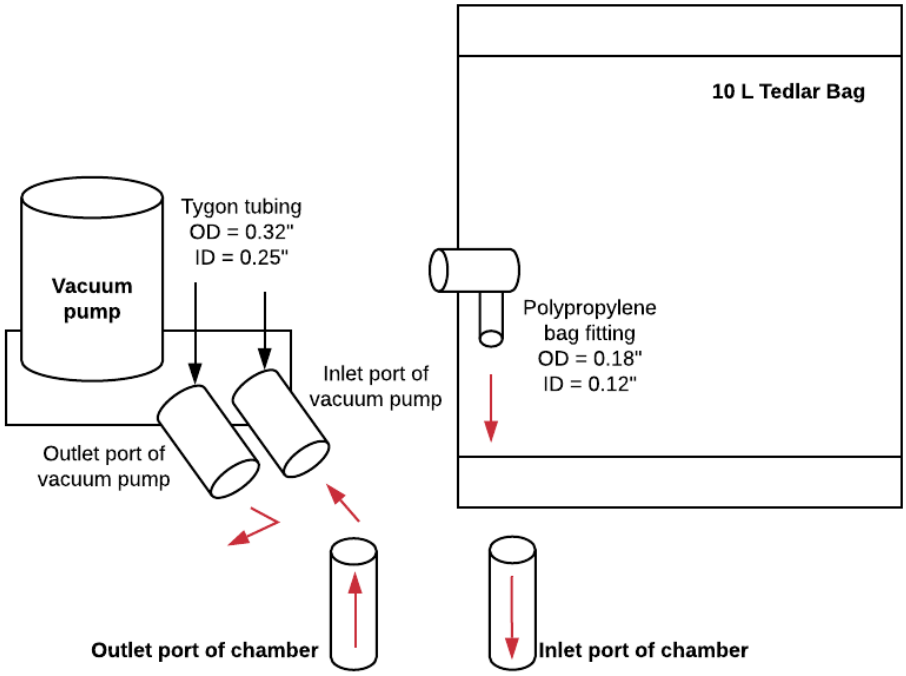

Figure 5. Diagram of chamber flushing setup with gas flow from the gas sample bag to the chamber followed by the vacuum pump represented by the red arrows

The polypropylene bag fitting was connected to the inlet port of the chamber and the inlet port of the vacuum pump was connected to the outlet port of the chamber. The on/off valves were opened, and the pump was turned on to allow gas flow from the gas sample bag through the chamber and through the vacuum pump. When the bag was nearly empty, the vacuum pump was shut off then the on/off valves of the chamber ports were closed immediately to stop the flow of gas. This was repeated for each incubation chamber until six of the chambers were flushed with 100% N_2, six were flushed with

approximately 90% N_2 and 10% O_2, and the remaining six were flushed with approximately 80% N_2 and 20% O_2.

2.5 Incubation Procedure

2.5.1. Gas Sampling

Fifty milliliters of gas were extracted from each of the eighteen incubation chambers every two to three days (sampling schedule available in **Error! Reference source not found.**). Each chamber was removed from the oven and shaken for approximately three seconds to facilitate gas mixing. A 50 mL syringe was attached to the chamber outlet, the on/off valve on the outlet was turned to allow for gas flow, and the syringe was filled with chamber gas. The on/off valve was then closed, and the chamber was returned to the oven to maintain incubation temperature for the designated treatment.

Syringe contents were divided to allow for analysis using both instruments (the gas chromatograph and GHG analyzer). A 20 mL aliquot was extracted from each gas sample syringe for determination of O_2 concentration through the Micro GC. The remaining gas in each syringe passed through the GHG Analyzer for determination of CO_2, CH_4, and N_2O concentrations.

2.5.2. Gas Replacement

Following gas extraction from the chambers for gas sample analysis, replacement gas was injected using a 50 mL syringe in order to maintain gas volume inside the chamber environment. The ratio of O_2 to N_2 in the replacement gas was calibrated to return the chamber to its original experimental O_2 concentration. This ratio was determined using the ideal gas law, $PV = nRT$ (Equation 2).

$$PV = nRT$$

Equation 2

where:

P = chamber pressure (atm) = 1.00 atm

V = gas volume in chamber (L); estimated using chip density and mass[a]

n = moles of O_2 required in chamber headspace for desired oxygen level[b]

R = gas constant (0.08205746 L · atm/mol · K)

T = incubation temperature (K)[c]

An intermediate calculation for the moles of O_2 required for the contents of each gas replacement syringe was done using the moles of oxygen required in the headspace (based on oxygen concentration for each respective treatment and chamber headspace volume), and the moles of oxygen in the chamber (based on the chamber headspace

[a] Chamber headspace volumes in this study ranged from 0.628-0.706 L
[b] (0%, 10%, or 20%)
[c] (293.15 K = 20°C, 313.15 K = 40°C, or 333.15 K = 60°C)

volume and the oxygen concentration of the sample as measured by the Micro GC) (Equation 3). Using PV = nRT and n_1-n_2 = n allowed for determination of oxygen volume (in L) that was required to return the chamber gas to the initial oxygen treatment (additional details for these calculations are provided in

Appendix G). The remaining volume (out of the 50 total milliliters removed for each sample) was taken up by addition of 100% nitrogen gas. The calculated amount of oxygen would be measured using syringes then injected into the chamber inlet port. The volume of nitrogen that would restore the total gas volume in the chamber was then added through the same inlet port, closing the valve in between injections to keep gas in the chamber from mixing with ambient air.

$$n_1 - n_2 = n$$

Equation 3

where:

n_1 = total moles of oxygen in chamber needed for treatment (0%, 10%, or 20%)

n_2 = moles of oxygen in chamber[d]

$n =$ moles of oxygen to be added to chamber through gas replacement

As soon as gas replacement was complete for a chamber, it was returned to the laboratory oven to maintain a consistent incubation temperature. On average, each chamber was outside of the laboratory oven for approximately ten minutes.

2.6 Energy Content Testing

Oxygen bomb calorimetry was used to compare the energy content of the feedstock before and after incubation. This was done to determine potential effects of the

[d] This value is calculated using readings from the gas chromatograph

incubation treatments of this study on the biomass feedstock. The instruments used for this procedure were the Parr 1241 Adiabatic Oxygen Bomb Calorimeter (Moline, IL) and the Parr 1108 Oxygen Combustion Bomb (Moline, IL). Diagrams of these materials are in

Appendix F.

2.6.1. Fuel Preparation

After the end of the incubation period, wood chips from the incubation chambers were oven dried at 105°C overnight (based on the ASTM Test Method for Moisture Analysis of Particulate Wood Fuels) then ground into fine particles using a coffee grinder. Approximately 5 grams of ground chips from each of the three replicate chambers in each of the six incubation treatments were mixed together to create a sample that was representative of the feedstock in each incubation treatment. Approximately 1 gram of dried feedstock sample was measured and added to a clean crucible for placement in the oxygen combustion bomb.

2.6.2. Oxygen Bomb Preparation

A length of fuse wire (approximately 10 cm, corresponding to about 23 calories) was cut and weighed. This length of wire was threaded through the terminals of the lid to the oxygen bomb by twisting the two ends and covering them with the attached metal sleeves. The crucible (with the measured biomass feedstock inside) was placed securely into the loop electrode of the bomb lid. The suspended fuse wire was then bent to ensure insertion into the feedstock sample. This assembled bomb lid and screw cap were placed onto the bomb cylinder and tightened by turning clockwise.

The gas supply valve of an oxygen tank fitted with a pressure regulator was opened. The pressure regulator valve was used to pressurize the bomb to 25 atm of pure

oxygen. The valve was closed when this pressure was obtained then disconnected from the bomb.

2.6.3. Water Bath Preparation

The mass of the water reservoir of the oxygen bomb calorimeter was measured to the nearest hundredth of a gram and recorded. Exactly 2000. grams of distilled water were added to the reservoir. The water temperature was adjusted to approximately 25°C. The reservoir was placed back into the calorimeter, with the base grooves aligned to the notches inside the calorimeter cavity.

2.6.4. Bomb Calorimetry Procedure

The bomb was placed into the middle of the water reservoir using pliers to avoid making physical contact with the water. The electrodes of the bomb calorimeter were plugged into the terminal nuts of the oxygen bomb. The electrode leads were then tucked towards the front face of the calorimeter to minimize risk of interference with the calorimeter stirrer. The calorimeter was closed, then the apparatus holding the thermometers and stirrer was lowered.

At this point, the calorimeter was set to ‘Run’ mode. The reservoir and jacket temperatures (indicated by the thermometers in the calorimeter) were monitored until equalization (within 0.02 °C). The initial temperature of the reservoir was recorded, then the ‘Ignite’ button was depressed from behind the window of the calorimeter enclosure. The maximum reservoir temperature was recorded as the final temperature and the calorimeter was turned off.

The thermometers, stirrer, and lid were moved aside to access the calorimeter cavity. The bomb was removed using pliers and dried with a towel. Under a laboratory fume hood, the pressure relief valve was opened slightly to allow oxygen to escape for approximately one minute. The lid was unscrewed, and the oxygen bomb was inspected for residue, indicating unburned feedstock and consequently the need for the test to be repeated. The excess fuse wire bits that were attached to the electrodes were removed and weighed. The oxygen bomb and the crucible were cleaned with deionized water and dried for subsequent tests. This procedure was repeated until three replicates of each incubation treatment were obtained.

2.6.5. Energy Content Calculations

The energy content (MJ kg^{-1}) of the feedstock samples was calculated using Equation 4.

$$E = \frac{Q}{m_{fuel}} = \frac{W(T_f - T_i)}{m_{fuel}}$$

Equation 4

where:

E = energy content of fuel (MJ kg^{-1})

Q = heat released (MJ)

m_{fuel} = mass (dry weight) of fuel consumed (kg)

W = calorimeter calibration constant (1.009×10^{-2} MJ K^{-1})[e]

T_f = maximum temperature of reservoir (°C)

T_i = initial temperature of reservoir (°C)

[e] The calibration constant can be calculated by combusting benzoic acid pellets (energy content = 26.43 MJ kg^{-1})

CHAPTER 3. RESULTS

Gas concentrations as reported by the GHG analyzer were used to measure emissions of each gas (CO_2, CH_4, N_2O). The average concentrations of each of these gases within each incubation treatment differed by orders of magnitude, with CO_2 concentrations being the greatest ($\leq$ 234,000 ppm), followed by CH_4 concentrations ($\leq$ 15 ppm) and N_2O ($\leq$ 6.0 ppm).

One noteworthy result of this study is the detection of CH_4 concentrations above ambient levels (~2 ppm) (NOAA, 2005). The peak CH_4 concentration detected was approximately 15 ppm, which was observed for the 60°C/20% O_2/70% moisture treatment. Other treatments at 60°C also yielded above-ambient levels of CH_4. These levels of CH_4 indicate that these incubation experiment conditions, which were informed by conditions within actual biomass piles, were conducive to methane generation.

Average gas concentration data by incubation treatment for each gas are in

Appendix H. Concentration values have been rounded according to the standard error of the regression for each gas during calibration calculations. Energy content results are in Appendix I. Figures 6-8 show the average gas concentrations of samples taken from each of the six distinct incubation treatments taken over the course of the biomass incubation for each temperature used in this study. These figures display the gas concentration plots for CO_2, CH_4, and N_2O, respectively. Error bars in each figure show one standard error (equal to the standard deviation of the concentrations by incubation treatment divided by the square root of the number of sampling events) in each direction.

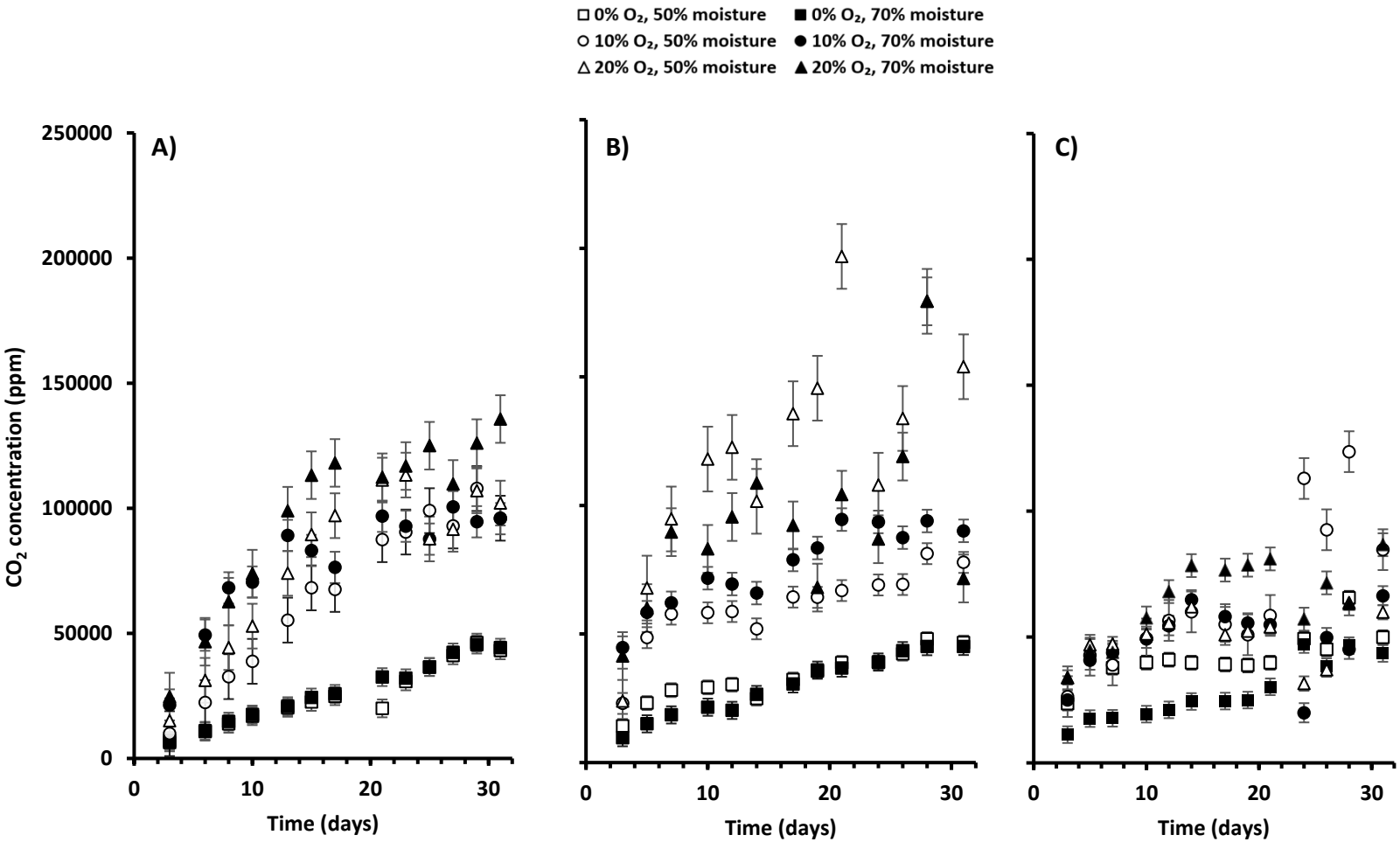

Figure 6. Average CO_2 concentrations over time by incubation treatment at 20°C (A), 40°C (B), 60°C (C), n = 3. Error bars represent ± 1 standard error.

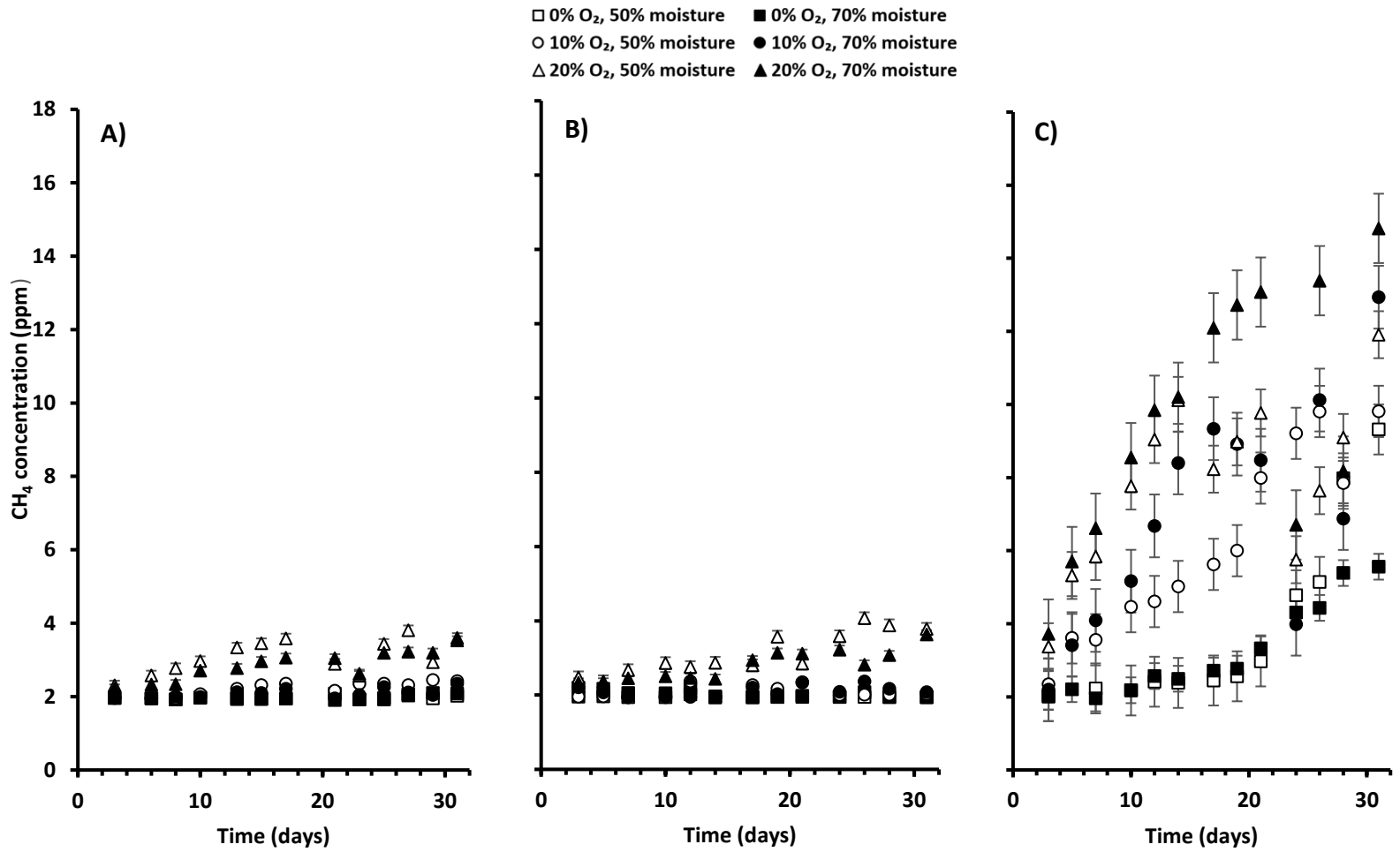

Figure 7. Average CH_4 concentrations over time by incubation treatment at 20°C (A), 40°C (B), 60°C (C), n = 3. Error bars represent ± 1 standard error.

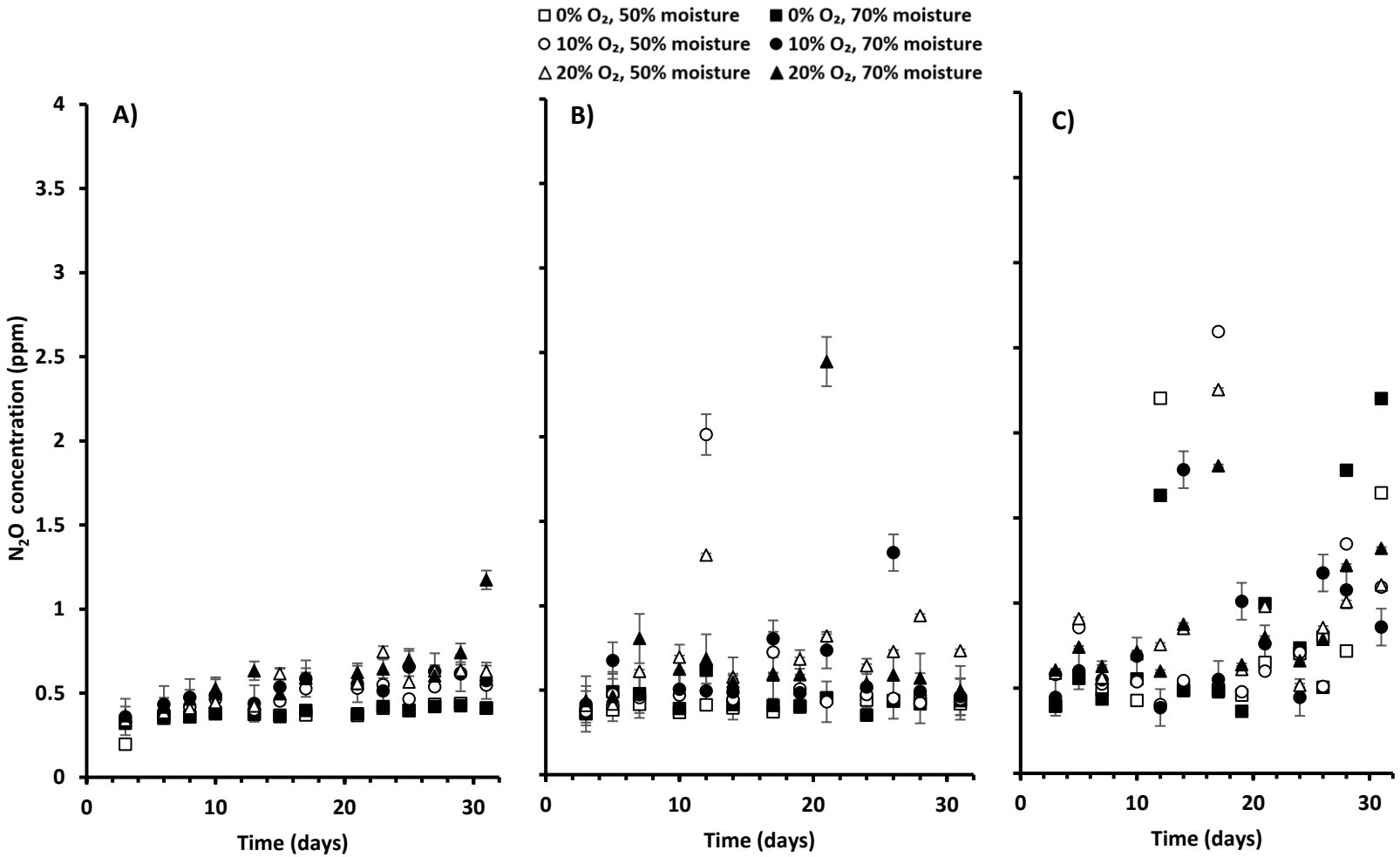

Figure 8. Average N_2O concentrations over time by incubation treatment at 20°C (A), 40°C (B), 60°C (C), n = 3. Error bars represent ± 1 standard error.

Table 2 displays the results of repeated measures analysis of variance (ANOVA) tests which were performed to investigate the differences in gas concentrations between treatments and among the variables included in this study. Variable effects are labeled with single terms (e.g. “Temp”) while variable interaction effects are labeled with multiple terms, separated by x’s (e.g. “Mois x Day”). Statistically significant differences are denoted with asterisks and a legend for the significance level of these differences is included at the bottom of the table.

Table 2. ANOVA results summary table

Gas	Variable	Df	MS	F	p
Carbon dioxide	Temp	1	5.03E+09	10.1	1.64E-03**
	Oxy	1	9.42E+08	1.91	1.69E-01
	Mois	1	6.17E+09	12.5	5.06E-04***
	Day	1	5.71E+10	116	< 2 E-16***
	Temp x Oxy	1	4.39E+07	8.90E-0.2	7.66E-01
	Temp x Mois	1	3.55E+08	0.719	3.98E-01
	Oxy x Mois	1	6.72E+07	0.136	7.13E-01
	Temp x Day	1	2.79E+09	5.65	1.83E-02*
	Oxy x Day	1	2.19E+08	0.444	5.06E-01
	Mois x Day	1	4.45E+08	0.901	3.44E-01
	Temp x Oxy x Mois	1	7.31E+07	0.148	7.01E-01
	Temp x Oxy x Day	1	6.15E+09	12.4	5.14E-04***
	Temp x Mois x Day	1	2.85E+07	5.8E-02	8.10E-01
	Oxy x Mois x Day	1	3.58E+08	0.724	3.96E-01
	Temp x Oxy x Mois x Day	1	6.11E+06	1.2E-02	9.12E-01
Methane	Temp	1	3.9E+00	1.7	1.99E-01
	Temp (not including 20°C)	1	6.1E+02	1.1E01	< 2 E-16***
	Temp (not including 40°C)	1	6.1E+02	1.1E01	< 2 E-16***
	Oxy	1	1.1E+01	4.8	2.90E-02*
	Mois	1	1.0E+01	4.5	3.54E-02*
	Day	1	7.4E+01	32	4.45E-08***
	Temp x Oxy	1	9.0E+00	4.0	4.76E-02*
	Temp x Mois	1	1.2E+01	5.4	2.10E-02*
	Oxy x Mois	1	1.0E-01	6.6E-02	7.97E-01
	Temp x Day	1	1.2E+02	51	1.27E-11***
	Oxy x Day	1	8.2E-01	0.36	5.48E-01
	Mois x Day	1	2.0E-01	8.6E-02	7.70E-01
	Temp x Oxy x Mois	1	7.3E-01	0.32	5.71E-01
	Temp x Oxy x Day	1	9.7E-01	0.43	5.14E-01
	Temp x Mois x Day	1	1.0E-03	1.0E-03	9.91E-01
	Oxy x Mois x Day	1	4.2E+00	1.9	1.74E-01
	Temp x Oxy x Mois x Day	1	3.1E-01	0.13	7.14E-01
Nitrous oxide	Temp	1	1.0E+00	3.4	6.63E-02
	Oxy	1	1.1E+00	3.8	5.42E-02
	Mois	1	2.8E-01	0.93	3.35E-01
	Day	1	6.9E-01	2.3	1.33E-01
	Temp x Oxy	1	2.7E-01	0.90	3.43E-01
	Temp x Mois	1	1.2E-01	0.41	5.25E-01
	Oxy x Mois	1	6.0E-04	2.0E-03	9.63E-01
	Temp x Day	1	7.1E-01	2.35	1.27E-01
	Oxy x Day	1	1.2E-02	3.9E-02	8.44E-01
	Mois x Day	1	6.9E-02	0.23	6.32E-01
	Temp x Oxy x Mois	1	2.8E-03	9.0E-03	9.23E-01
	Temp x Oxy x Day	1	3.4E-01	1.1	2.88E-01
	Temp x Mois x Day	1	4.2E-01	1.4	2.37E-01
	Oxy x Mois x Day	1	3.7E-01	1.2	2.69E-01
	Temp x Oxy x Mois x Day	1	7.1E-01	2.4	1.27E-01

Temp = Temperature, Oxy = Oxygen, Mois = Moisture

* $p < 0.05$; ** $p < 0.01$; *** $p < 0.001$

Cumulative CH_4 emissions are significantly different across temperature treatments and cumulative CO_2 and N_2O emissions are significantly different across oxygen treatments. Figures 9-11 show the average cumulative gas emissions produced per incubation treatment across the three incubation temperatures for CO_2, CH_4, and N_2O, respectively. Cumulative gas emissions were calculated by multiplying the gas concentration observed during each gas sampling event by the syringe volume and adding these values to the gas concentration observed during the final gas sampling event multiplied by the respective chamber gas volume (Equation 5). Cumulative gas emissions calculations resulted in maxima of 150 g CO_2 (± 5.04 g), 2E-02 g CH_4 (± 9E-04 g), and 2E-02 g N_2O (± 1E-02 g) of emissions from a given treatment type within this study. Results for cumulative gas emissions by chamber are in Appendix J.

$$Total\ emissions\ per\ chamber = C_f * V_c + \sum_{i=1}^{n} (C_i * V_s)$$

Equation 5

where:

C_f = concentration of final gas sample (g/L)

C_i = concentration of gas sample (g/L)

V_c = chamber headspace (L)

V_s = syringe volume (0.05 L)

n = number of gas sampling events

Error bars in Figures 9-11 represent one standard error in each direction. For convenience, the levels within each variable will be labeled as follows: low moisture (50% moisture), high moisture (70% moisture), low oxygen (0% O_2), medium oxygen (10% O_2), and high oxygen (20% O_2).

Figure 12 shows the average CH_4/CO_2 molar concentration ratio from the incubation treatments for the 20°C, 40°C, and 60°C incubation temperatures. Because the highest incubation temperature (60°C) tended to generate the greatest relative quantities of both CH_4 and CO_2 emissions (according to Figures 9 and 10), this CH_4/CO_2 ratio was calculated in order to investigate whether this ratio varied with temperature.

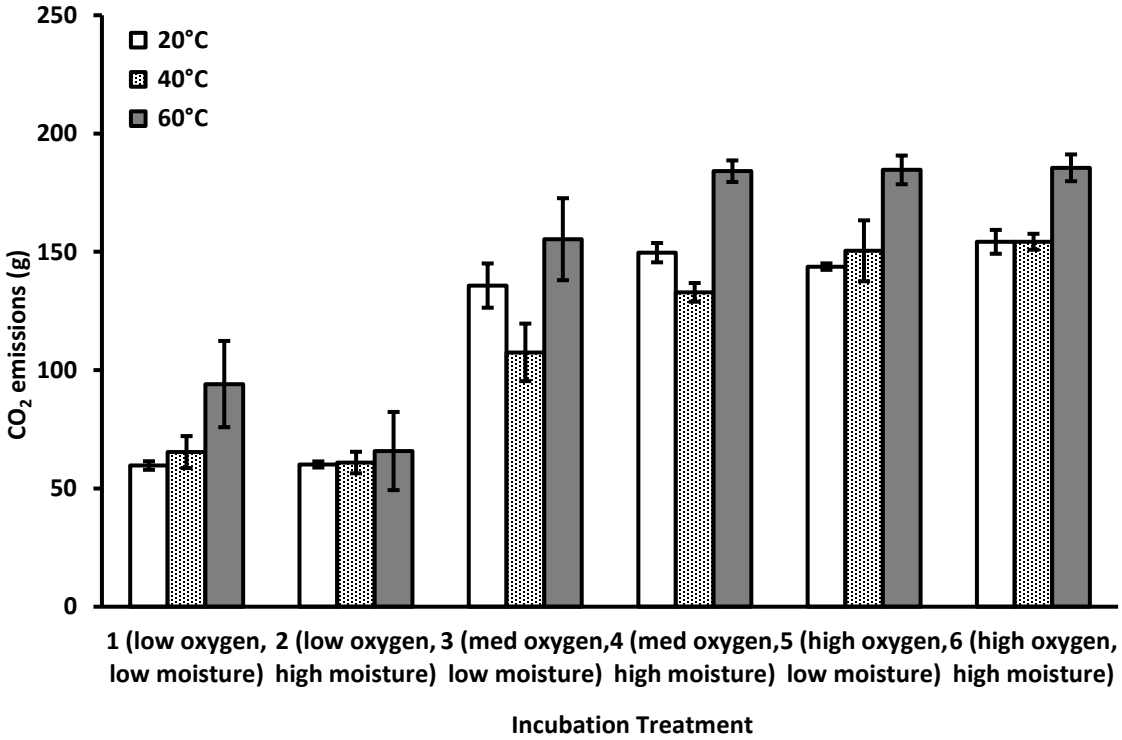

Figure 9. Total CO_2 emitted (g) over 30 days from each round of biomass incubation, separated by treatment, n = 3. Error bars represent ± 1 standard error.

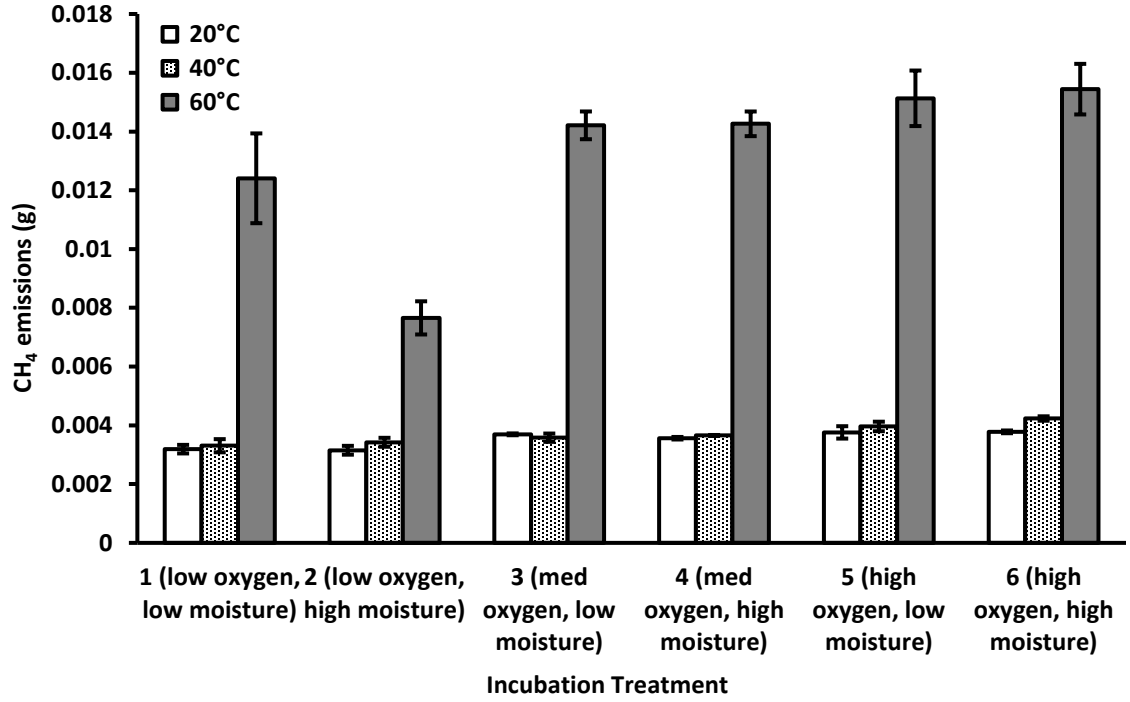

Figure 10. Total CH_4 emitted (g) over 30 days from each round of biomass incubation, separated by treatment, n = 3. Error bars represent ± 1 standard error.

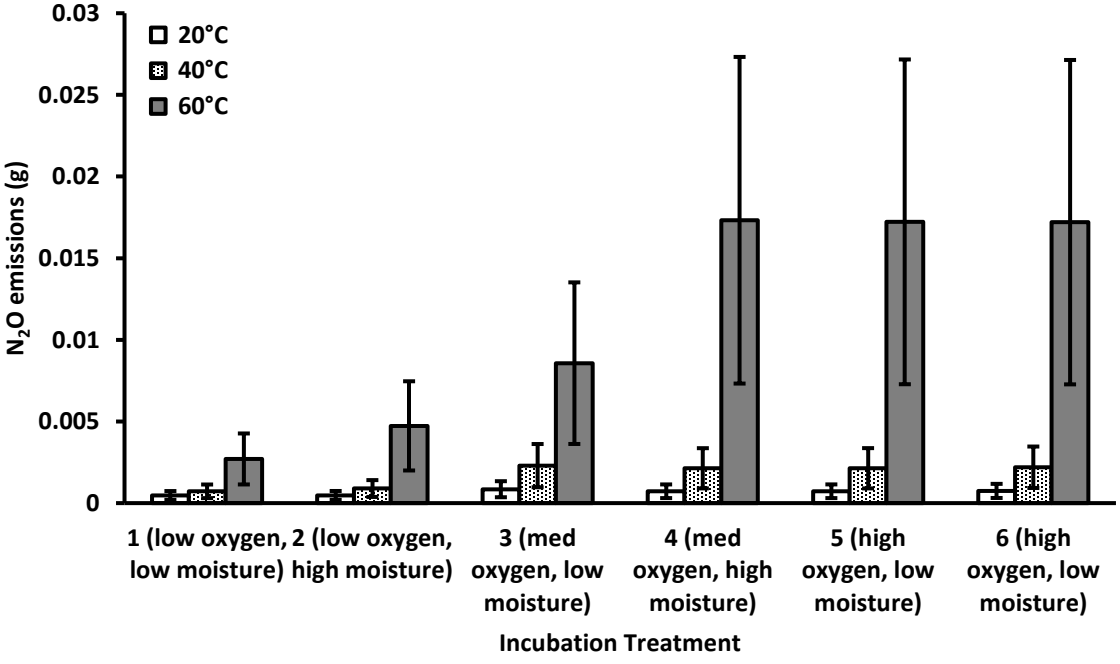

Figure 11. Total N_2O emitted (g) over 30 days from each round of biomass incubation, separated by treatment, n = 3. Error bars represent ± 1 standard error.

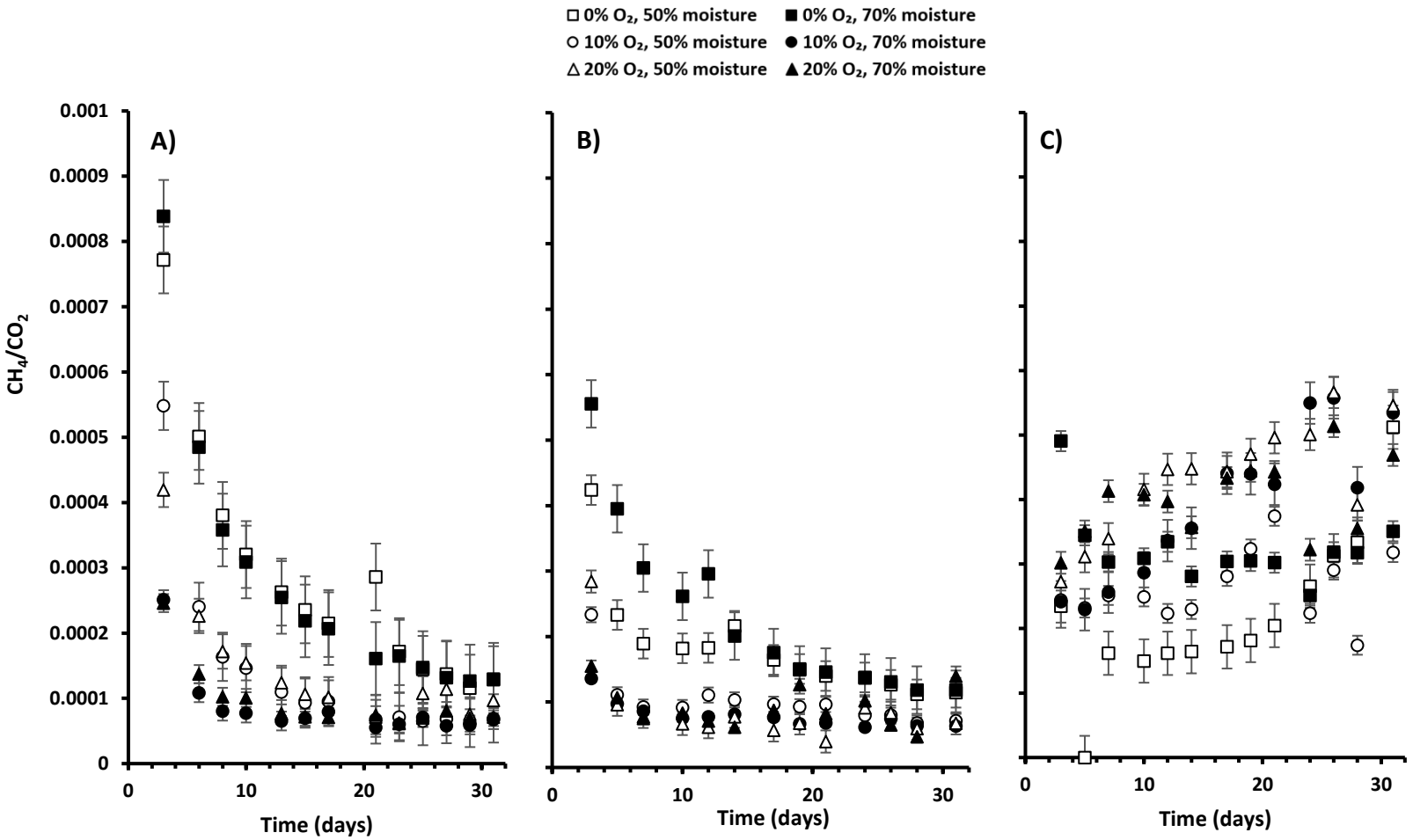

Figure 12. CH_4/CO_2 molar ratios in the incubation chambers over the incubation period at 20°C (A), 40°C (B), 60°C (C). Error bars represent ± 1 standard error.

Multiple linear regression was used to model total gas emissions per chamber (for each of the three gas species of interest) as a function of temperature, oxygen, and moisture. Multiple linear regression results for all three gases are shown in **Error! Reference source not found.**. Additional analyses were performed with only two of the three variables (either temperature and oxygen or temperature and moisture) for CO_2 and CH_4. These additional analyses were informed by the ANOVA results.

A regression equation for total CO_2 emissions was found ($F(3, 14) = 20.1$, $p < 0.001$), with an $R^2 = 0.771$. Predicted total CO_2 emissions can be calculated using Equation 6. Oxygen concentration and incubation temperature were significant predictors of total CO_2 emissions ($p < 0.001$ and $p < 0.05$, respectively).

A regression equation for total CH_4 emissions was also found ($F(3, 14) = 12$, $p < 0.001$), with an $R^2 = 0.7$. Predicted total CH_4 emissions can be calculated using Equation 7. Temperature was a significant predictor of total CH_4 emissions ($p < 0.001$).

Finally, a regression equation for total N_2O emissions was found ($F(3,14) = 8.8$, $p < 0.001$), with an $R^2 = 0.58$. Predicted total N_2O emissions can be calculated using Equation 8. Incubation temperature and oxygen treatment were significant predictors of total N_2O emissions ($p < 0.001$ and $p < 0.05$, respectively). Q-Q plots for the three analyses are found in

Appendix K.

Table 3. Results of multiple linear regression analyses by gas species (β = coefficient, β_0 = intercept, SE = standard error, SE_r = standard error of regression, df = degrees of freedom)

Gas	Predictor	β	SE	β_0 (g)	SE_r	df	F	p	adj. R^2
CO_2	Temp (°C)	6.93E-01 (g/°C)	3.18E-01	32.7	22.0	14	20.1	2.45E-05	0.771
	Oxy (%)	4.72E0 (g/%)	6.36E-01						
	Mois (%)	2.83E-01 (g/%)	5.20E-01						
	Temp (Temp x Oxy)	4.93E-01 (g/°C)	5.04E-01	57.7	22.1	14	20.0	2.49E-05	0.771
	Oxy (Temp x Oxy)	3.92E0 (g/%)	3.90E-02						
CH_4	Temp (°C)	2.4E-04 (g/°C)	4.1E-05	-2.6E-03	2.9E-03	14	12	3.7E-04	0.66
	Oxy (%)	1.1E-04 (g/%)	8.3E-05						
	Mois (%)	-2.3E-05 (g/%)	6.8E-05						
	Temp (Temp x Oxy)	1.8E-04 (g/°C)	6.3E-05	-1.6E-03	2.7E-03	14	14	2.0E-03	0.69
	Oxy (Temp x Oxy)	-1.2E-04 (g/%)	2.1E-04						
	Temp (Temp x Mois)	3.5E-04 (g/°C)	2.7E-04	-5.7E-03	3.0E-03	14	10	7.6E-04	0.62
	Mois (Temp x Mois)	4.8E-05 (g/%)	1.9E-04						
N_2O	Temp (°C)	2.7E-04 (g/°C)	5.8E-05	-1.2E-02	4.0E-03	14	8.8	1.6E-03	0.58
	Oxy (%)	2.5E-04 (g/%)	1.2E-04						
	Mois (%)	6.0E-05 (g/%)	9.4E-05						

Three additional analyses were performed to investigate CO_2 and CH_4 emissions as predicted by a combination of two variables rather than all three (the selected combinations were informed by the ANOVA results, Table 2 displays the results of repeated measures analysis of variance (ANOVA) tests which were performed to investigate the differences in gas concentrations between treatments and among the variables included in this study. Variable effects are labeled with single terms (e.g. “Temp”) while variable interaction effects are labeled with multiple terms, separated by x’s (e.g. “Mois x Day”). Statistically significant differences are denoted with asterisks and a legend for the significance level of these differences is included at the bottom of the table.

Table 2). Regression equations were found for CO_2 emissions as predicted by temperature and oxygen ($F(2, 14) = 20.1$, $p < 0.001$, $R^2 = 0.771$), CH_4 emissions as predicted by temperature and oxygen ($F(2, 14) = 14$, $p < 0.001$, $R^2 = 0.69$), and CH_4 emissions as predicted by temperature and moisture ($F(2, 14) = 10$, $p < 0.001$, $R^2 = 0.62$). Predicted emissions of CO_2 and CH_4 as outlined above can be calculated using Equations 9-11, respectively.

Total predicted CO_2 (g), as a function of temperature, oxygen, and moisture =

$$32.7 + (0.693T) + (4.72X) + (0.283M)$$

Equation 6

Total predicted CH_4 (g), as a function of temperature, oxygen, and moisture =

$$-2.60E\text{-}03 + (2.42E\text{-}04T) + (1.10E\text{-}04X) - (2.26E\text{-}05M)$$

Equation 7

Total predicted N_2O (g), as a function of temperature, oxygen, and moisture =

$$-1.22E\text{-}02 + (2.66E\text{-}04T) + (2.52E\text{-}04X) - (5.96E\text{-}05M)$$

Equation 8

Total predicted CO_2 (g), as a function of temperature and oxygen =

$$57.7 + (0.493T) + (3.92X)$$

Equation 9

Total predicted CH_4 (g), as a function of temperature and oxygen =

$$-1.63E\text{-}03 + (1.83E\text{-}04T) - (1.23E\text{-}04X)$$

Equation 10

Total predicted CH_4 (g), as a function of temperature and moisture =

$$\text{-}5.74\text{E-}03 + (3.48E\text{-}04T) - (4.80E\text{-}05M)$$

Equation 11

where:

T = temperature (°C)

X = oxygen concentration (%)

M = moisture content (%, wet basis)

Emission factors for each gas at the three incubation temperatures used for this study were calculated using Equation 12 (derived from Kuang et al., 2008). These emission factors, in addition to the peak gas concentrations and incubation time to reach the peak gas concentrations, are displayed in

Table 4.

$$f_{\propto} = \frac{P(C_i V) * M_{wt}}{RTM_p}$$

Equation 12

where:

$f_{\propto}$ = emission factor (g gas/kg woodchip mass)

P = chamber pressure (atm) [f]

C_i = peak/maximum gas concentration (g/L)

V = gas volume in chamber (L)

M_{wt} = gas molecular weight (g/mol)

R = gas constant (0.082057 L · atm/mol · K)

T = chamber temperature (K)

M_p = mass of chip material in chamber (kg) [g]

[f] Pressure was approximated as a constant of 1 atm based on observation of minimal changes in pressure during a test incubation period of woodchips at 60°C. This assumption has also been made in a related study (Kuang et al., 2008) which reports a maximum pressure increase of 6.9-8.1 kPa (0.068-0.079 atm) for incubation of Douglas fir woodchips at 50°C over the course of 60 days.

[g] The mass of chip material in each incubation chamber of this study is available in Appendix C. The values are representative of wet weight.

Table 4. Peak raw gas concentrations (C_p), incubation time to reach peak concentrations (T_p), and emission factors ($f_\propto$) of gases emitted from woody biomass during incubation at different temperatures and oxygen concentrations

Variable		CO_2			CH_4			N_2O		
T (°C)	O_2 (%)	C_p (ppm)	T_p (day)	$f_\propto$ (g/kg)	C_p (ppm)	T_p (day)	$f_\propto$ (g/kg)	C_p (ppm)	T_p (day)	$f_\propto$ (g/kg)
20°C	0%	48,000	29	0.348	3	21	6.4E-03	0.5	29	3.4E-03
	10%	133,600	21	0.965	3	25	7.7E-03	1.0	29	8.1E-03
	20%	213,000	26	1.67	5	31	1.3E-03	2.0	31	1.8E-02
40°C	0%	55,600	28	0.380	3	2	6.7E-03	1.0	11	7.4E-03
	10%	113,600	28	0.790	3	25	7.4E-03	4.0	11	2.6E-02
	20%	292,600	29	2.03	5	31	1.3E-02	6.0	22	4.4E-02
60°C	0%	90,200	10	0.645	14	31	3.2E-02	2.0	21	1.3E-02
	10%	156,600	28	1.07	19	31	4.5E-02	2.0	21	1.3E-02
	20%	100,400	21	0.611	17	31	4.1E-02	2.0	5	1.4E-02

CHAPTER 4. DISCUSSION

The following sections are organized by the three major topics of this study: 1) the effects of variable environmental factors on greenhouse gas emissions, 2) the cumulative greenhouse gas emissions from this incubation study, and 3) the generation of predictive models for these greenhouse gas emissions. Within each topic, the discussion breaks down further into each respective gas (CO_2, CH_4, and N_2O). The final section of this chapter highlights limitations of the study described herein.

4.1 Effect of Temperature on GHG Emissions

Results from the repeated measures ANOVA tests (Table 2 displays the results of repeated measures analysis of variance (ANOVA) tests which were performed to investigate the differences in gas concentrations between treatments and among the variables included in this study. Variable effects are labeled with single terms (e.g. “Temp”) while variable interaction effects are labeled with multiple terms, separated by x’s (e.g. “Mois x Day”). Statistically significant differences are denoted with asterisks and a legend for the significance level of these differences is included at the bottom of the table.

Table 2) demonstrate that only CO_2 emissions from woody biomass incubation differ statistically significantly by temperature ($p < 0.005$). These emissions also differ significantly by the interaction between temperature and time ($p < 0.05$) and between temperature, oxygen, and time ($p < 0.001$). These results pair well with the plots displaying CO_2 concentration over time (Figure 6). All three panels of Figure 6 show steady increases over time in CO_2 concentration. Panel C (showing the high temperature treatment, 60°C) seems to show less dramatic concentration increases when compared with panels A and B. While multiple studies on woody biomass decomposition report that greater temperatures tend to enhance gaseous emissions (He et al., 2011; Alakoski et al., 2015; Kuang et al., 2008), this finding suggests that the relative amount of CH_4 emissions versus CO_2 emissions increases as a function of increased temperature (Alakoski et al., 2015; Kuang et al., 2008). The plots of CH_4/CO_2 molar ratios over time (Figure 12) display a difference between the ratio trend in panel C and in panels A and B (representative of 60°C, 40°C, and 20°C, respectively). The molar ratio of CH_4 to CO_2 increases gradually for the 60°C treatment, while the ratios decrease steadily and appear to asymptotically approach 0 for the 40°C and 20°C treatments.

Combined, these results suggest that CH_4 generation is favored over CO_2 generation at 60°C. An increase in the proportion of decomposition which occurs anaerobically over aerobically indicates a shift in microbial population as temperature increases; evidence from previous studies indicate the presence of thermophilic microorganisms in wood chip piles (Adams and Frostick, 2009; Noll and Jirjis, 2012).

The plots of CH_4 concentration over time (Figure 7) display a stark difference between concentrations observed at 60°C and the lower temperature treatments. CH_4 concentrations increased sharply and consistently over time at this high temperature treatment, but at the lower temperatures (40°C and 20°C) CH_4 concentrations increased only slightly above ambient concentrations of approximately 2 ppm CH_4 (NOAA, 2005). The peak CH_4 concentration detected in this study was approximately 15 ppm, which was observed for the 60°C/20% O_2/70% moisture treatment. Detecting above-ambient levels of CH_4 alone was a notable finding. The experimental conditions chosen for this incubation study were informed in part by measurements taken at an actual woodchip storage pile. This indicates that when this combination of environmental conditions is present in a storage pile, methane generation may be expected.

The anaerobic conditions that allow for methane generation may be present due to higher biological decomposition rates driven by higher temperature. The significant difference in CH_4 concentrations across temperature treatments may also imply that some threshold exists between 40°C and 60°C that prompts substantial growth of methanogenic microorganisms. This observation agrees with the conclusions of Noll and Jirjis (2012), which suggest that a majority of mesophilic fungus species favor environments of 30-40°C while thermophilic fungi (a group which includes many methanogens) are known to thrive up to approximately 60°C.

These CH_4 concentration findings in relation to temperature are well-supported by the ANOVA results (Table 2) that show that CH_4 emissions were found to differ significantly by the interaction of temperature and oxygen ($p < 0.05$), temperature and

moisture ($p < 0.05$), and temperature and day ($p < 0.001$). Two additional ANOVA tests were conducted to investigate the potential of a significant difference between the concentrations at 60℃ and either 40℃ or 20℃, since the latter two temperatures yielded similar CH_4 concentrations, so the three-way ANOVA did not show a significant difference between CH4 concentrations by temperature ($p > 0.1$). The two-way t-tests showed significant differences between CH_4 concentrations at 60℃ and 40℃ and between concentrations at 40℃ and 20℃ (both resulted in $p < 0.0001$). The results here further support the relationship between increased incubation temperature and increased production of CH_4. These CH_4 concentrations across temperature treatments may also suggest a shift in the composition of the microbial community that lived on and in the woodchip material, favoring anaerobic decomposition over aerobic decomposition. The detection of CH_4 in these chambers suggests that the study conditions led to rates of decomposition that were high enough to cause oxygen depletion in portions of the sample material.

ANOVA results (Table 2 displays the results of repeated measures analysis of variance (ANOVA) tests which were performed to investigate the differences in gas concentrations between treatments and among the variables included in this study. Variable effects are labeled with single terms (e.g. “Temp”) while variable interaction effects are labeled with multiple terms, separated by x’s (e.g. “Mois x Day”). Statistically significant differences are denoted with asterisks and a legend for the significance level of these differences is included at the bottom of the table.

Table 2) indicate that N_2O concentrations did not differ statistically significantly across temperature treatments ($p > 0.05$). Additionally, there were no statistically significant interactions between the effects of temperature and other environmental factors that influence N_2O concentration. The plots of N_2O concentrations (Figure 8) do not show meaningful changes over time, except for a slight increasing trend around day 26 for the concentrations recorded from the 60℃ treatment. A greater length of incubation might allow for improved observation of N_2O generation by biomass decomposition. This investigation could be of great interest due to the high global warming potential of N_2O and the possibility of significant levels of emissions occurring after the study incubation period of 30 days. Apart from this observation, most gas sample N_2O concentrations tended to fluctuate around ambient levels of approximately 0.335 ppm (NOAA, 2005). Similarly, N_2O concentrations were undetected or detected at very low concentrations in similar studies (Whittaker et al., 2017; Alakoski et al., 2016).

4.2 Effect of Oxygen Concentration on GHG Emissions

The availability of oxygen is linked directly to the production of CO_2 via oxidation (Meier et al., 2016). Several studies support this concept (Alakoski et al., 2016; Meier et al., 2016; He et al., 2014). For example, a previous study by He et al. (2014) reports a distinct halt in CO_2 generation following the depletion of O_2 in study reactors (used to incubate Douglas fir woodchips).

ANOVA results indicate that oxygen treatment does not explain CO_2 concentrations ($p > 0.05$). Relative CO_2 emissions decrease as the temperature increases as a result of conditions that favor anaerobic decomposition (**Error! Reference source not found.**).

According to the ANOVA results, oxygen treatment level had a statistically significant effect on CH_4 concentration ($p < 0.05$). Points representing average CH_4 concentrations found at 0% O_2 tend to remain lower in the plots, while points representing average concentrations at 20% O_2 appear to be relatively high (Figure 7). Concentration values appear to remain relatively low for treatments at 0% O_2 and vice versa for 20% O_2. Panels A and B show data that do not differ much across oxygen treatments. These CO_2 concentration results are supported by the statistically significant interaction between oxygen concentration and temperature ($p < 0.05$) as it relates to CH_4 concentrations. In summary, increased oxygen concentrations are conducive to greater CH_4 emissions, and this effect may be most easily observed when rates of decomposition are high enough to allow for the creation of anaerobic micro-environments within a mass of feedstock. It may be the case that in the chamber environment, an initially high O_2 concentration facilitated relatively high rates of biological decomposition which resulted in a shorter duration of time for the chamber to be depleted of O_2.

Data suggest that oxygen concentration did not have a statistically significant effect on N_2O concentration ($p > 0.05$). The extremely low levels of N_2O generation reported in this study may not allow for proper investigation of this gas. Perhaps a longer

total incubation time or a greater mass of woodchips per chamber would be beneficial in examining drivers of N_2O emissions.

Energy content testing using samples from two treatments at the 20°C level and unincubated chips resulted in similar values (20.1 MJ/kg ± 1.50E-02 MJ/kg, 19.6 MJ/kg ± 0.198 MJ/kg, and 19.1 MJ/kg ± 0.223 MJ/kg for samples at 20°C/50% moisture/0% O_2, 20°C/50% moisture/20% O_2, and unincubated samples at 50% moisture, respectively). The values are very close, with the first group resulting in the greatest energy content and unincubated material resulting in the least energy content, which is not expected based on the connection between dry matter loss and decreasing energy content. There are statistical differences between the groups, and this may be due to variation in the feedstock. Greater clarity around this difference could be obtained with a greater sample size.

Efforts were made to maintain oxygen concentrations within incubation chambers at the specified levels for each treatment of this study (0%, 10%, or 20%). Changes in O_2 concentrations were observed over time (

Appendix L) and the overlap between the observed O_2 concentrations for these treatments is greater than would be desired. This observation may be due to some combination of faults in the chamber design and gross error. Conclusions drawn from the relationship between oxygen concentrations and gas emissions are therefore limited. Further discussion on this topic is found at the end of this chapter (Section

4.6 Limitations).

One aspect of the study design that likely impacted the changing O_2 values in chambers is the time interval at which gas samples were collected from the chambers. In this study, samples were extracted every 2-3 days: sampling schedule available in **Error! Reference source not found.**. The He et al. (2014) study on incubation of Douglas fir woodchips reports O_2 concentration dropping to 0% in the three highest temperature treatments (20℃, 35℃, 50℃) "at the beginning of the test". Their gas emission profile results indicate that oxygen depletion was observed within the first 10 days of the 60-day incubation period, and a drop of approximately 8% O_2 over the course of 3 days was observed for the 50℃ treatment (He et al., 2014). Injection of replacement gas could not completely compensate for this high rate of change within the chamber environment; the O_2 concentration fluctuated as much as 10.7% over a single time interval, which is greater than the differences in the selected oxygen concentration treatments themselves (0%, 10%, 20%). Future experiments could consider a shorter time interval between gas sampling and/or a greater difference between selected O_2 levels for an incubation study. A mechanism for monitoring the O_2 levels in each chamber would be ideal for this aspect of the study.

4.3 Effect of Moisture Content on GHG Emissions

Moisture content had a highly statistically significant effect on CO_2 concentrations ($p < 0.001$). The data representing treatments with 70% moisture content

and 0% O_2 treatment generally have the lowest gas concentrations and therefore lowest rates of emissions. Although the trend is inconsistent, higher moisture treatment (70%) seems to result in lesser CO_2 concentrations over time (Figure 6).

The effect of moisture in this study counters previous studies reporting the relationship between moisture content and gas emissions from biomass decomposition. High moisture content is reported to cause greater rates of dry matter loss, resulting in decreased heating value and consequently, adverse effects on the bioenergy supply chain (Sahoo et al., 2018; Jamsen et al., 2015; Whittaker et al., 2016). Decreasing the moisture content to 20% (wet basis) or lower is recommended in order to slow the decomposition process (Jamsen et al., 2015).

That higher moisture was associated with decreased decomposition in this study may be due to the relatively high moisture content used here. The typical range of moisture content in harvested biomass reported by Whittaker et al. (2016) is 40-60%, and the greater of the two moisture levels for this incubation study was 70% (wet basis). This level was selected to investigate gas emissions associated with biomass decomposition in waterlogged or highly saturated conditions as a result of heavy precipitation or inadequate drainage at the biomass storage site. Less attention has been paid to the effects of moisture content on the higher end of the spectrum as compared with the lower end, which is preferable due to expected savings in GHG emissions and in operational costs (Whittaker et al., 2016). It may be the case that microbial activity is inhibited by the effects of moisture content greater than 60% due to decreased pile porosity and therefore diminished flow of gas throughout the chip material (Jamsen et al., 2015). Additionally, a

greater proportion of the pores in the woodchip tissue would be occupied by water at higher moisture levels, making it easier for the O_2 to be depleted.

Moisture had a significant effect on CH_4 concentrations ($p < 0.05$). CH_4 concentrations were higher in chambers at the 70% moisture level than for their counterparts at the 50% moisture level within each of the three oxygen treatments (Figure 7). This association – between higher moisture and higher gas emission – is in keeping with the negative relationship between moisture content and potential gas flow, since CH_4 generation is associated with anaerobic decomposition. This suggests that woodchip piles with higher moisture contents (such as those formed outdoors, especially when uncovered) may produce greater relative amounts of CH_4.

ANOVA results indicate that the effect of moisture on N_2O concentrations was not significant. This pairs well with the N_2O concentration plots over time, which display no discernable trend with respect to moisture levels.

One additional complication in relation to the N_2O data is the sensitivity of the GHG analyzer, which must operate within a specific range of pressure in order to function as programmed. During the course of the experiment, there were several drops (followed immediately by spikes) in N_2O concentrations, which caused the analyzer to report negative concentration values for some gas samples. A technical support scientist from Picarro Inc. was able to remotely diagnose the problem by relating these abnormal concentration readings with cavity pressure of the GHG analyzer. The outlet valve closed during sample delivery in order to return to optimal operating pressure. This change was likely due to the specific method of sample delivery used in this study, which involved

attaching syringe tips to the inlet of the GHG analyzer and allowing the GHG analyzer pump to evacuate the syringe contents prior to manual detachment of the syringe. To remedy this problem, the study protocol was adjusted to prioritize prompt removal of the sampling syringes in order to minimize or eliminate time during which the GHG analyzer would experience pressure-induced fluctuations.

4.4 Cumulative GHG Emissions and Emission Factors

Calculated cumulative CO_2 emissions suggest that incubation at 60℃ yields more greenhouse gas emissions from woody biomass decomposition than incubation at 40℃ or 20℃. Total CO_2 emissions for treatments at 60℃ were greater than CO_2 emissions for treatments at 40℃ and 20℃ within each treatment group, with statistically significant differences in these totals present 0% O_2/50% moisture, 10% O_2/70% moisture, 20% O_2/50% moisture, and 20% O_2/70% moisture. Total emissions increase as O_2 concentration increases, though concentrations from treatment 4 (at 10% O_2) do not differ significantly from concentrations recorded for treatments 5 and 6 (20% O_2).

The emission factors for CO_2 range from 0.348 – 2.03 g gas/kg wet weight of biomass over one month (

Table 4). Emission factors were calculated for the treatments of the incubation study by a matrix of 3 x 3 (oxygen x temperature), omitting the relatively minor differences by moisture content. He et al. (2014) report emission factors of approximately 2.75 g/kg wet woodchips over two months for treatments ranging from 20-50°C.

Kuang et al. (2008), who developed the emission factor equation, report a maximum of 0.106 g CO_2/kg wet biomass. The difference in magnitude between this reported value and the values from this study is likely due to the difference in biological composition of the study feedstock. Kuang et al. utilized wood pellets from pine trees harvested approximately 2 years after felling (2008). This feedstock age, as well as the low moisture content associated with the pellets (~4%), would be expected to yield relatively low rates of decomposition.

According to Andersen et al. (2010), a CO_2e emission factor above 20 g/kg material would indicate poorly managed biomass storage. Calculations from this study show that emission factors for CO_2 range from 0.348 – 2.03 g gas/kg wet weight of biomass. The emission factors for CH_4 and N_2O are orders of magnitude lower than those for CO_2 and therefore would contribute very little towards CO_2e emission factors (

Table 4). While the factors calculated here are far below the suggested threshold, it is worth noting that the length for which biomass piles are on site (and left undisturbed) is often much longer than the length of this study (~30 days), and emissions could be impacted by a multitude of factors in situ. Further research is needed to contribute to the understanding of CO_2e emissions from storage in these conditions.

For cumulative CH_4 emissions, for each of the six treatments, there is a statistically significant difference between total emissions observed at 60℃ and total emissions observed at 40℃ and 20℃ (**Error! Reference source not found.**). High temperatures are associated with higher methane emissions. This finding is also illustrated in Figure 7, showing the methane concentration over time; here, the methane concentrations for the highest temperature significantly exceed the concentrations for the other lower temperature treatments. Moisture content does not have a significant effect on total CH_4 emissions, except in the case of a comparison between data representative of treatments 1 and 2 (0% O_2/50% moisture and 0% O_2/70% moisture) at 60℃. Whittaker et al. (2016) report CH_4 emissions between 0.04 – 2.2 g/kg for a woodchip storage pile over three months. The maximum calculated emission factor for this study is 4.5E-02 g CH_4/kg chip material, which lies on the low end of that range.

Total N_2O emissions, displayed in **Error! Reference source not found.**, suggest that temperature is a significant factor. From lowest to highest oxygen concentrations, the total N_2O emissions increase as well. No significant difference is observed with treatments 3, 4, 5, and 6 at 40℃ and 20℃.

The relationship found between N_2O emissions and temperature runs counter to findings from previous literature-- nitrifying bacteria are sensitive to temperatures above 40°C and meaningful N_2O emissions are not expected above this threshold (Wilhersaari, 2005; Alakoski et al., 2016). Nitrous oxide emissions are generally expected at the beginning and end of the storage phase, when the temperature is relatively low (Jamsen et al., 2015). The deviation between this study's findings and previous literature may be possible due to a combination of some or all of the following factors: 1) nitrous oxide may be formed via nitrification during aerobic decomposition or denitrification during anaerobic decomposition, causing fluctuations in generation rates, 2) nitrogen content of biodegradable material is variable and it may be the case that the feedstock used in this study differs in this respect when compared with previous studies' feedstock, and 3) the chamber environment may have created an environment that resulted in unnaturally low rates of gas mixing, creating pockets of anaerobic decomposition that would not have been formed in an actual pile setting (Jamsen et al., 2015). These factors may also have implications for the generation of other greenhouse gases, especially those that are generated in anaerobic conditions such as methane.

The greatest emission factor calculated for N_2O in this study was 0.043 g/kg chip material over one month of storage. Previous research on emissions associated with biomass storage has generally focused on CO, CO_2 and CH_4. Two studies have reported N_2O emission factors that bracket those found in the literature, and underline the uncertainty of this estimate; Andersen et al. (2010) report an emission factor of 0.331 g N_2O/kg organic household waste, and Hansen et al. (1994) report an emission factor of

0.717 g N_2O/kg pig solid slurry. Although woody biomass emissions tend to be much lower than emissions from other organic materials in general, decomposition occurs on a longer time scale (Jamsen et al., 2015). Considerations with respect to feedstock material must be made in quantifying emissions and eventually making decisions around management of biomass storage.

4.5 Predictive Models of Emissions

Multiple linear regression was performed for emissions of each of the three GHGs in this study to explore the effect of a combination of two to three incubation study variables on the total mass of emissions of each gas (Equations 5-10). Most relationships between predictors and gas emissions were positive, indicating that increases in temperature, oxygen concentration, and moisture generally lead to a predicted increase in gas emissions. There was a decrease of 1.23E-04 g (± 2.09E-04) in the CH_4 emissions for every 1% increase in O_2 concentration when analyzing the effects of temperature and oxygen only (**Error! Reference source not found.**), however, this interval includes both negative and positive values, making this an inconclusive result.

Regression equations for CO_2 (including the additional analysis of temperature and oxygen only) resulted in models with $R^2 > 0.77$, indicating a substantial proportion of the variance in emissions explained by the models. Regression equations for CH_4 (including the additional analyses of temperature and oxygen only, and temperature and moisture only) resulted in models with $R^2 = 0.62\text{-}0.69$, indicating that over 60% of the

variance in CH_4 emissions explained by the models. Excluding moisture as an explanative variable resulted in a model with a higher fraction of explained variance (relative to the model with all three variables).

The regression equation for N_2O as predicted by all three variables resulted in $R^2 = 0.580$, indicating 58% of the variance in N_2O emissions was explained by the models. All together, these equations seem to supply a prediction for GHG emissions when given the three environmental variables used in this study. The null hypothesis, which concludes that some combination of these environmental factors is not likely to influence total gas emissions, can be rejected because the p-value results are low for all analyses ($p < 0.001$). As will be discussed in the following section, however, scalability of these equations and applications to larger contexts is questionable due to inherent differences between laboratory incubation studies and field studies.

4.6 Limitations

Calculated emission factors for the three gases investigated in this study fit reasonably well with emission factors reported in previous studies and any discrepancies can generally be explained by findings from previous studies about the behavior of biological or chemical decomposition. Biological decomposition, driven by microbial metabolism, is studied indirectly here via the measurement of the concentrations of GHGs. A better understanding of the biological decomposition processes may be obtained through a combination of these measurements and observation of the actual species of microorganisms present within the feedstock samples before, during, and after incubation. It was outside the scope of the present study to include microbial culture methods, but this could be of interest for a future study. Findings that combined results from observed gas emissions and a deep understanding of the present microbial community composition within the feedstock material were not available in the literature.

Expected rates of oxygen depletion were calculated based on reported values from previous studies. Observed rates were generally greater than these expected rates. The time intervals between sampling events (and consequently, gas mixture replacement within the chambers) were two to three days. For a relatively small incubation chamber which is meant to house a microcosm of a biomass pile region, this proved to be plenty of time for changes in O_2 concentration.

Potential sources of error involving the incubation chambers themselves should be acknowledged. There were a few chamber lids that needed repairs during incubation

(specifically, three chamber lids during the first round of incubation, which subjected chambers to the highest temperature, 60°C); small holes (< 5 mm) were detected while sampling events occurred. These were patched as soon as they were observed. In cases where the holes were not successfully patched, the incubation chamber was pulled from the experiment and a new one was assembled to take its place. Before incubation, all chambers were individually tested for leaks. Gas syringes were used for injection and extraction tests using multiple times the syringe volume to replicate the effects of gas production and gas sampling, respectively. A liquid leak detector (Snoop from Swagelok Co.) was used to visualize leaks via the formation of bubbles. Every chamber that was utilized for the study passed the leak test (no leaks detected after 600 mL of gas injection and also after extraction of 180 mL). It is hypothesized that the incubation treatments created corrosion conditions that compromised some of the materials of the chamber lids and caused the creation of these small holes over time.

Additionally, there were a few incidents during gas sampling events that resulted in either an inlet or outlet port of a chamber being opened accidentally. These incidents did not last for longer than a couple seconds, as they were caused by movement of relatively loose on/off valves associated with the ports during transfer of chambers to/from the inside of the laboratory oven.

Finally, the reliability of these results is limited by the operating range of the GHG analyzer. A large majority (approximately 75%) of the recorded CO_2 concentrations were out of the suggested operating range of the instrument. According to Picarro, the maximum CO_2 concentration that the GHG analyzer is guaranteed to

measure is 2% (20,000 ppm). Because results from the first round of incubation (at 60°C) included concentrations above this threshold, re-calibration was performed with the addition of a gas standard at a higher concentration of CO_2 (110,000 ppm) than used previously. Observed concentrations of CO_2 over the course of the study surpassed this value as well, and consequently there are data that lie outside of the range of calibration.

CHAPTER 5. CONCLUSIONS AND RECOMMENDATIONS

The main objectives of this thesis are 1) observing the effects of variable environmental factors on greenhouse gas emissions (CO_2, CH_4, and N_2O) from incubation of woody biomass feedstock, 2) measuring the cumulative greenhouse gas emissions from this incubation study, and 3) generating a predictive model for these greenhouse gas emissions. Based on the results obtained from this incubation study, it can be concluded that the temperature, oxygen concentration, and moisture content have statistically significant effects on the decomposition of woody biomass and therefore on the composition of the generated emissions. The results in this study are generally in accord with findings from the available published literature. Supported theories regarding biomass decomposition and related mechanisms can be applied to the context of this incubation study to help in understanding any unexpected results.

Results from this study suggest that CO_2 emissions from woody biomass decomposition are dependent on O_2 availability and are significantly influenced by variation in temperature and in moisture content of the biomass material. The combination of the temperature and O_2 concentration over time has a significant effect on the production of CO_2 emissions. The peak CO_2 concentration detected in the study was approximately 235,000 ppm (which was observed for the 40°C/20% O_2/50% moisture treatment). While the data from this study may be skewed due to CO_2 concentrations outside the operating range of the GHG analyzer, there is reasonable confidence in these high readings, due to adjustments made in calibration.

The greatest concentrations of CO_2 were previously expected at 60°C based on the commonly reported correlation between temperature and dry matter loss, which results in greater associated emissions. This was not observed here and may be partially explained by the CH_4/CO_2 molar ratio, which increases over time at 60°C, while at 40°C and 20°C, this ratio drops and asymptotically approaches 0.

CH_4 emissions from woody biomass vary significantly across temperature. The CH_4 emissions observed at 60°C were significantly greater than emissions at 40°C and 20°C, suggesting a potential threshold somewhere between 40°C and 60°C at which conditions become more favorable for methanogenic microorganisms. Concentrations at 20°C and 40°C remained close to ambient levels (~2 ppm). The peak CH_4 concentration detected in the study was approximately 15 ppm (which was observed for the 60°C/20% O_2/70% moisture treatment).

Extremely low observed concentrations of N_2O in this study were expected, based on results from previous work. Most concentrations tended to fluctuate around ambient levels (~0.3 ppm). No significant effects of temperature, O_2 concentration, or moisture content were found. Lack of significant effects may be due to the relatively high variation in N_2O concentrations, which may be due in part to the sample delivery method and associated fluctuations in the pressure-sensitive instrument cavity of the GHG analyzer.

Cumulative gas emissions calculations resulted in maxima of 154 g CO_2 (± 5.04 g), 1.5E-02 g CH_4 (± 8.6E-04 g), and 1.7E-02 g N_2O (± 9.9E-03 g) of emissions from a given treatment type within this study. Models were generated via multiple linear regression to predict gaseous emissions of CO_2, CH_4 and N_2O as a function of the three

incubation study variables (or some combination of two of the variables). These had relatively high proportions of variance in total emissions explained by the proposed models ($R^2 > 0.77$ for CO_2 models, $R^2 > 0.62$ for CH_4 models, and $R^2 > 0.57$ for N_2O models). These may be useful in quantifying potential GHG emissions from storage of woody biomass and performing a cost-benefit analysis of storage operations.

Several incubation studies have made contributions to the knowledge base regarding emissions associated with biomass decomposition. Valuable insight can be obtained with the high levels of control associated with lab-based studies such as those performed by Kuang et al. (2008), Meier et al. (2016), He et al. (2014), all of which helped inform the methodology for the study described herein. Caution should be used in applying these findings to actual storage pile conditions, since there may be unexpected implications to scaling models and values such as emission factors. Additionally, these incubation studies (by design) exclude a whole host of factors which are known to impact rates of decomposition and dry matter loss for outdoor storage of woodchips, including local precipitation, woodchip particle size, feedstock species, and in situ pile dynamics such as ventilation and the “chimney effect”.

Studies that focus on GHG emissions from biomass are crucial to assessing the impacts of many modern processes, including the combustion of woody biomass for production of energy. This study has focused on specific GHG emissions from *S. sempervirens* during an incubation period with different treatments of temperature, oxygen concentration, and moisture content in order to shed light on the influence of these environmental factors (and the interaction of these factors) on woody biomass

decomposition. This approach was motivated by the understudied storage phase of the bioenergy supply chain, which may be contributing significantly to the overall carbon flux of large-scale biomass utilization. Further studies are required to build on the current understanding of these decomposition processes in order to properly assess the feasibility of these technologies and ultimately the efficacy of bioenergy as a method of waste management and source of renewable energy.

Potential improvements to this study are numerous. With additional time and resources, a similar study which utilizes more levels within the environmental variables, more replicates per treatment, and greater sampling frequency could be performed. Monitoring of internal chamber pressure, moisture, and oxygen content would also be ideal. A longer incubation period would also allow for better comparison to field-scale studies.

While continued research in this incubation setting would be valuable for fine-tuning the understanding around the effects of certain environmental variables, it makes sense to move into field studies to test the scalability of these results. Large systems for monitoring and/or controlling these variables (temperature, oxygen concentration, and moisture content) should be employed in this case. It would be useful to study more storage piles that are on-site for utilization at plants and refineries.

Finally, a closer look at the microorganisms present before, during, and after incubation would be of great interest. Investigating the variety of species and observing the “shifts” in composition could be a way of linking the emissions and the environmental conditions. It was outside the scope of this study to include microbial

culture methods, but this could be a crucial aspect of understanding the mechanisms behind the observed gaseous products during biomass decomposition.

REFERENCES

Adams, J.D.W, and L. E. Frostick. 2009. "Analysis of Bacterial Activity, Biomass and Diversity during Windrow Composting." *Waste Management (Elmsford)* 29: 598-605.

Afzal, M., A. Bedane, S. Sokhansanj, W. Mahmood. 2010. “Storage of Comminuted and Uncomminuted Forest Biomass and its Effect on Fuel Quality.” *Bioresources* 51:55-69.

Alakoski, E., M. Jamsen, D. Agar, E. Tampio and M. Wilserhaari. 2015. "From wood pellets to wood chips, risks of degradation and emissions from the storage of woody biomass – A short review." *Renewable and Sustainable Energy Reviews* 54:376-383.

Andersen, J. K, A. Boldrin, J. Samuelsson, T. H. Christensen, and C. Scheutz. 2010. "Quantification of Greenhouse Gas Emissions from Windrow Composting of Garden Waste." *Journal of Environmental Quality* 39: 713-24.

Andersen, J. K., A. Boldrin, T. H. Christensen, and C. Sheutz. 2010. "Greenhouse Gas Emissions from Home Composting of Organic Household Waste." *Waste Management* 30: 2475-482.

Anerud, E., S. Krigstin, J. Routa, H. Brännström, M. Arshadi, C. Helmeste, D. Bergström, G. Egnell. 2019. “Dry matter losses during biomass storage: measures to minimize feedstock degradation.” *IEA Bioenergy*.

American Standard of Testing and Materials. 2006. “Standard Test Method for Moisture

Analysis of Particulate Wood Fuels.” ASTM International E871-82.

Barbose, G. 2018. “U.S. Renewables Portfolio Standards: 2018 Annual Status Report.” *U.S. Renewables Portfolio Standards: 2018 Annual Status Report | Electricity Markets and Policy Group*, emp.lbl.gov/publications/us-renewables-portfolio-standards-1.

Bedane, A, M. Afzal, and S. Sokhansaj. 2011. "Simulation of temperature and moisture changes during storage of woody biomass owing to weather variability." *Biomass and Bioenergy* 35:3147-3151.

California Energy Commission. 2019. “California Biomass and Waste-To-Energy Statistics and Data.” *California Biomass and Waste-To-Energy Statistics and Data*, https://ww2.energy.ca.gov/almanac/renewables_data/biomass/index_cms.php.

Chen, H., M. Harm, R. Griffiths, and W. Hicks. 2000. "Effects of Temperature and Moisture on Carbon Respired from Decomposing Woody Roots." *Forest Ecology and Management* 138.1: 51-64.

Covey, K., and J. Megonigal. 2019. Methane production and emissions in trees and forests. New Phytologist, 222: 35–51.

Hansen, M. N, K. Henriksen, and S. G. Sommer. 1994. "Observations of Production and Emission of Greenhouse Gases and Ammonia during Storage of Solids Separated from Pig Slurry: Effects of Covering." *Atmospheric Environment* 40: 4172-4181.

He, X., A. Lau, A., S. Sokhansanj, C. Jim Lim, X. Bi, S. Melin. 2012. "Dry matter losses in combination with gaseous emissions during the storage of forest residues."

Fuel 95:662-664.

He, X., A. Lau, S. Sokhansanj, C. Jim Lim, X. T. Bi, S. Melin. 2014. "Investigating gas emissions and dry matter loss from stored biomass residues." *Fuel* 134:159-165.

Inficon. 2013. “Reference Guide: 3000 Micro GC Gas Analyzer.”

Jamsen, M., D. Agar, E. Alakoski, E. Tampio, M. Wilhersaari. 2015. "Measurement methodology for greenhouse gas emissions from storage of forest chips–A review." Renewable and Sustainable Energy Reviews 51:1617-1623.

Jenkins, B., R. Williams, N. Parker, P. Tittmann, Q. Hart, M. Gildart, S. Kaffka, B. Hartsough, and P. Dempster. 2009. “Sustainable use of California biomass resources can help meet state and national bioenergy targets.” California Agriculture 63:10.

Jirjis R and O. Theander. 2008. The effect of seasonal storage on the chemical composition of forest residue chips, Scandinavian Journal of Forest Research, 5:1-4, 437-448.

Kuang, X., T. Shankar, X. Bi, S. Sokhansanj, C. Lim, S. Melin. 2008. "Characterization and kinetics study of off-gas emissions from stored wood pellets." *The Annals of Occupational Hygiene* 52:675–683.

Kuang, X., T. Shankar, X. Bi, C. Lim, S. Sokhansanj, and S. Melin. 2009. Rate and peak concentrations of off-gas emissions in stored wood pellets--sensitivities to temperature, relative humidity, and headspace volume. *The Annals of Occupational Hygiene*, *53*(8), 789-796.

Lottes, A. 2014. Supply chain and process emissions impact of torrefaction to enable

biomass in large power plants versus raw biomass use in small power plants. Master's Thesis. Humboldt State University.

Mayhead, G. and P. Tittmann. 2012. "Uncertain future for California's biomass power plants." California Agriculture 66(1):6.

Meier, F., I. Sedlmayer, W. Emhofer, E. Wopienka, C. Schmidl, W. Haslinger, and H. Hofbauer. 2016. "Influence of Oxygen Availability on Off-Gassing Rates of Emissions from Stored Wood Pellets." *Energy & Fuels* 30.2: 1006-012.

Mobini, M, J. Meyer, F. Trippe, S. Frederik, F. Taraneh, F. Schultmann. 2014. "Assessing

the Integration of Torrefaction into Wood Pellet Production." *Journal of Cleaner Production* 78: 216-25.

Noll, M., and Jirjis, R. 2012. Microbial communities in large-scale wood piles and their effects on wood quality and the environment. Applied Microbiology And Biotechnology, 95(3), 551-563.

Pecenka, R., H. Lenz, and C. Idler. 2018. "Influence of the chip format on the development of mass loss, moisture content and chemical composition of poplar chips during storage and drying in open-air piles." *Biomass and Bioenergy* 116:140–150.

Picarro. 2018. "G2508 Analyzer Datasheet." https://www.picarro.com/support/library/documents/g2508_analyzer_datasheet_data_sheet

Pier, P. A., and J. M. Kelly. 1997. "Measured and Estimated Methane and Carbon Dioxide Emissions from Sawdust Waste in the Tennessee Valley Under

Alternative Management Strategies." *Bioresource Technology* 61:213-220.

Sahoo, K., Bilek, E.M., and Mani, S. 2018. "Techno-economic and Environmental Assessments of Storing Woodchips and Pellets for Bioenergy Applications." *Renewable & Sustainable Energy Reviews* 98: 27-39.

Sommer, S., S.M. McGinn, X. Hao, and F.J. Larney. 2004. "Techniques for Measuring Gas Emissions from a Composting Stockpile of Cattle Manure." *Atmospheric Environment* 38.28: 4643-652.

Svedberg, U. R. A., H. Högberg, J. Högberg, B. Galle. 2004. "Emission of Hexanal and Carbon Monoxide from Storage of Wood Pellets, a Potential Occupational and Domestic Health Hazard." *The Annals of Occupational Hygiene* 48.4: 339. Web.

Thörnqvist, Thomas. 1985. “Drying and storage of forest residues for energy production.” *Biomass* 7:125-134.

U.S. Department of Commerce, NOAA. “Global Monitoring Laboratory - Carbon Cycle Greenhouse Gases.” *NOAA Earth System Research Laboratories*, 1 Oct. 2005, www.esrl.noaa.gov/gmd/ccgg/trends_ch4/.

U.S. Energy Information Administration (EIA) “Independent Statistics and Analysis.” *Electricity in the U.S. - U.S. Energy Information Administration (EIA)*, 2019, www.eia.gov/energyexplained/electricity/electricity-in-the-us.php.

Whittaker, C., N. Yates, S. J. Powers, N. Donovan, T. Misselbrook, I. Shield. 2017. "Testing the Use of Static Chamber Boxes to Monitor Greenhouse Gas Emissions from Wood Chip Storage Heaps." *Bioenergy Research* 10: 353-62.

Whittaker, C., N. Yates, S. J. Powers, T. Misselbrook, I. Shield. 2016. "Dry Matter Losses and Greenhouse Gas Emissions from Outside Storage of Short Rotation Coppice Willow Chip." *Bioenergy Research*; New York 9:288-302.

Wihersaari, M. 2005. "Evaluation of Greenhouse Gas Emission Risks from Storage of Wood Residue." *Biomass & Bioenergy* 28: 444-53.

APPENDICES

Appendix A. Field observations

To help parameterize the variables (temperature, oxygen concentration, and moisture content) of this incubation study, conditions observed at an active biomass power plant were recorded. These values, in combination with reported values from previous studies, were used to inform the selection of levels within the variables of the study. A power plant in the northwestern region of the United States, which uses 335,000 tons of recovered wood debris and residues annually, permitted a field visit in 2019 during which samples of woodchips were collected, gas samples within the feedstock piles were collected, and temperature measurements at various depths of feedstock piles were taken.

A variety of woodchip samples were collected for laboratory testing. Sample locations from the selected piles differed in age and in depth. Three out of nine samples were taken from a pile aged approximately 4-6 months (Pile A) and extracted from 5 feet into the pile. Another set of three samples were taken from a pile aged 3 weeks (Pile B) and extracted from 9 feet into the pile. The last set of samples were also taken from Pile B, from the pile surface.

A temperature probe was constructed to measure inner pile temperatures on-site, up to a depth of approximately 6.5 feet. The recorded temperatures increased as the depth of the probe increased, suggesting that the center of the pile is the hottest and therefore is

the most metabolically active. The highest pile temperature recorded during this visit was approximately 71°C.

Three gas samples were collected from Pile A at different depths. These samples were analyzed using the Micro GC. The trend in oxygen concentration was found to initially decrease as the depth increases, but an unexpected increase in concentration was found at roughly 9 feet into the pile, where the value rose from 12% to 19% of gas volume. The CO_2 concentration dropped from about 5% at a depth of 6 feet to 2% at a depth of 9 feet.

Moisture content was measured using the Standard Test Method for Moisture Analysis of Particulate Wood Fuels, issued by ASTM International. The moisture content values varied from 27.9% to 55.3%, with the "newer" Pile B samples tending to have higher moisture than the Pile A samples. This was expected, as woodchips in storage lose water over time via evaporation. The older Pile A material had an average moisture content of 33.2% at a depth of 5 ft. The Pile B samples, collected from both the pile surface and a depth of nine feet, had average moisture content values of 45.4% and 52.5%, respectively.

These results help to create a general idea of the existing trends in the feedstock piles. Because of the small sample size, these results are not to be considered statistically significant. The tests, however, have been beneficial in parameterizing and shaping the experimental design for the laboratory study described herein.

Appendix B. Pictures of lab materials

Figure B1. Picture of open incubation chamber with woodchips

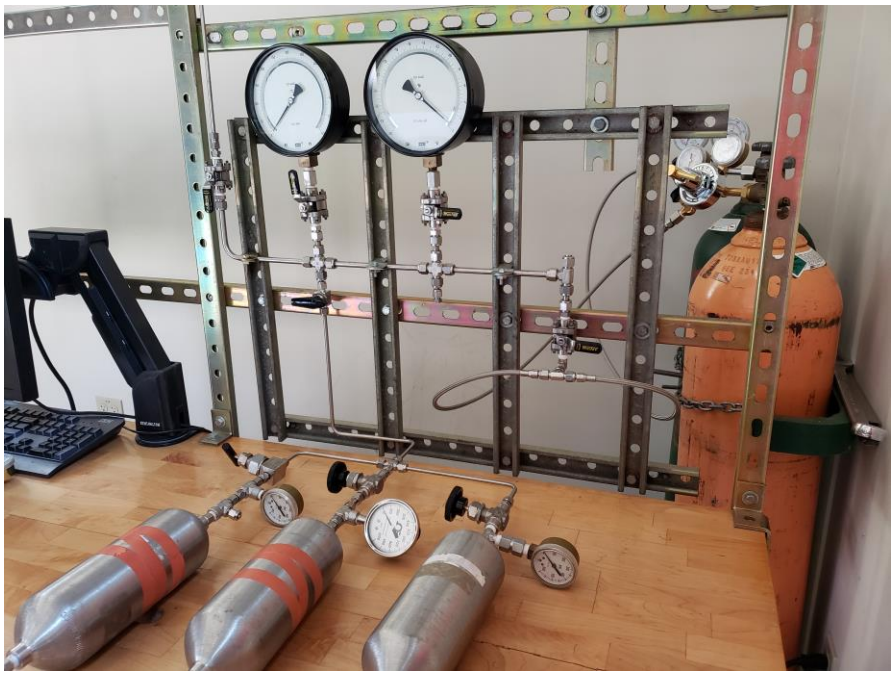

Figure B2. Picture of gas mixing manifold

Figure B3. Picture of sample material (with U.S. penny for scale)

Appendix C. Calibration results for GHG analyzer

Table C1. Calibration results for carbon dioxide, methane, and nitrous oxide. S_e = standard error of the regression. Numbers shown for analyzer's reported concentration are an average of three replicates (n = 3).

Gas Species	Calibration Point	Analyzer's Reported Concentration (ppm)	Concentration of Gas Standard (ppm)	S_e (ppm)
CO_2	1	720.54	725	150.
CO_2	2	1885.23	2000	150.
CO_2	3	86404.93	110000	150.
CH_4	1	4.5	5	0.822
CH_4	2	10.58	10	0.822
CH_4	3	14.61	15	0.822
N_2O	1	10.6	10	0.260
N_2O	2	50.9	50	0.260
N_2O	3	407	400	0.260

$$y = 1.28x - 300$$

Eq. C1 (calibration curve for CO_2)

$$y = 0.976x + 0.343$$

Eq. C2 (calibration curve for CH_4)

$$y = 0.983x - 0.251$$

Eq. C3 (calibration curve for N_2O)

Appendix D. Woodchip mass data

Table D1. Wood chip mass per chamber for each of the three incubation rounds

	Mass (g)	Mass (g)	Mass (g)
Chamber	Round 1 (60℃)	Round 2 (40℃)	Round 3 (20℃)
1	169	151	151
2	155	155	146
3	144	154	154
4	153	179	187
5	154	180	187
6	150	179	178
7	144	151	152
8	157	152	158
9	153	151	147
10	176	174	184
11	162	179	187
12	160	179	176
13	185	151	143
14	179	151	141
15	164	150	149
16	179	178	174
17	170	177	169
18	161	179	172

Appendix E. Gas sampling schedule

Table E1. Table of gas sampling schedule for incubation study

	Round 1 (60 °C)	Round 1 (60 °C)	Round 2 (40 °C)	Round 2 (40 °C)	Round 3 (20 °C)	Round 3 (20 °C)
Sampling Event	Date	Day	Date	Day	Date	Day
Start	3/14/2020	0	5/4/2020	0	6/16/2020	0
1	3/16/2020	2	5/6/2020	2	6/19/2020	3
2	3/18/2020	4	5/8/2020	4	6/22/2020	6
3	3/20/2020	6	5/11/2020	7	6/24/2020	8
4	3/23/2020	9	5/13/2020	9	6/26/2020	10
5	3/25/2020	11	5/15/2020	11	6/29/2020	13
6	3/27/2020	13	5/18/2020	14	7/1/2020	15
7	3/30/2020	16	5/20/2020	16	7/3/2020	17
8	4/1/2020	18	5/22/2020	18	7/7/2020	21
9	4/3/2020	20	5/25/2020	21	7/9/2020	23
10	4/6/2020	23	5/27/2020	23	7/11/2020	25
11	4/8/2020	25	5/29/2020	25	7/13/2020	27
12	4/10/2020	27	6/1/2020	28	7/15/2020	29
13	4/13/2020	30	6/3/2020	30	7/17/2020	31

Appendix F. Diagrams of oxygen bomb calorimetry materials

PARTS FOR THE 1241 ADIABATIC CALORIMETER

Key No.	Part No.	Description
1	A332DD2	Stirrer lift bracket
2	A270DD3	Thermometer clamp
3	A455DD	Thermometer bracket w/latch
4	A459DD	Safety rod assembly
5	245DD	Thermtr. bracket support rod
6	A323DD	Cover lift assembly
7	243DD2	Cover lift roller
8	SR1214	Roll pin
9	292DD	Drive belt
10	A355DD	Stirrer assembly, complete
11	251DD	Lift disc w/set screw & pin
12	239DD	Stirrer pulley with screw
13	357DD	Bearing hub
14	356HC	Snap ring, large
15	196A	Spring
16	354HC	Ball bearing (2 req'd.)
17	417DD	Sealing ring (2 req'd.)
18	A237DD	Stirrer shaft w/propellers
19	A162E	Motor w/pulley, mtg. plate & cplg.
20	498DD	Coupling with set screws
21	A506DD	Pump impeller assembly
22	A423DD	Pump tube assembly
23	A380DD2	Pump collar assembly
24	483DD	O-ring
25	272DD	Thermometer support rod
26	365DD	Thermistor fitting
27	A364DD	Thermtr. fittg. w/422DD ring
28	A391DD	Calorimeter bucket
29	The following parts are required to replace the calorimeter jacket and/or cover:	
	A376DD2	Jacket assby. w/bucket supports
	A428DD	Cover assembly
	A380DD2	Pump support collar assby.
	A423DD	Pump tube assembly
	A506DD	Pump impeller assembly
	A323DD	Cover lift assembly
	A243DD2	Cover lift roller
	SR1214	Roll pin
	438DD	O-ring
	A364DD	Thermometer fitting
	365DD	Thermistor fitting
	A162E	Motor w/pulley, mtg. plate & cplg.
30	A300E3	Control panel assembly
31	A297E	Lead wire w/banana plug (2 req'd.)
32	A403DD	Water control panel assby.
33	A135VB	Flow control valve
34	A406DD	Metering valve
35	89HW	Solenoid valve

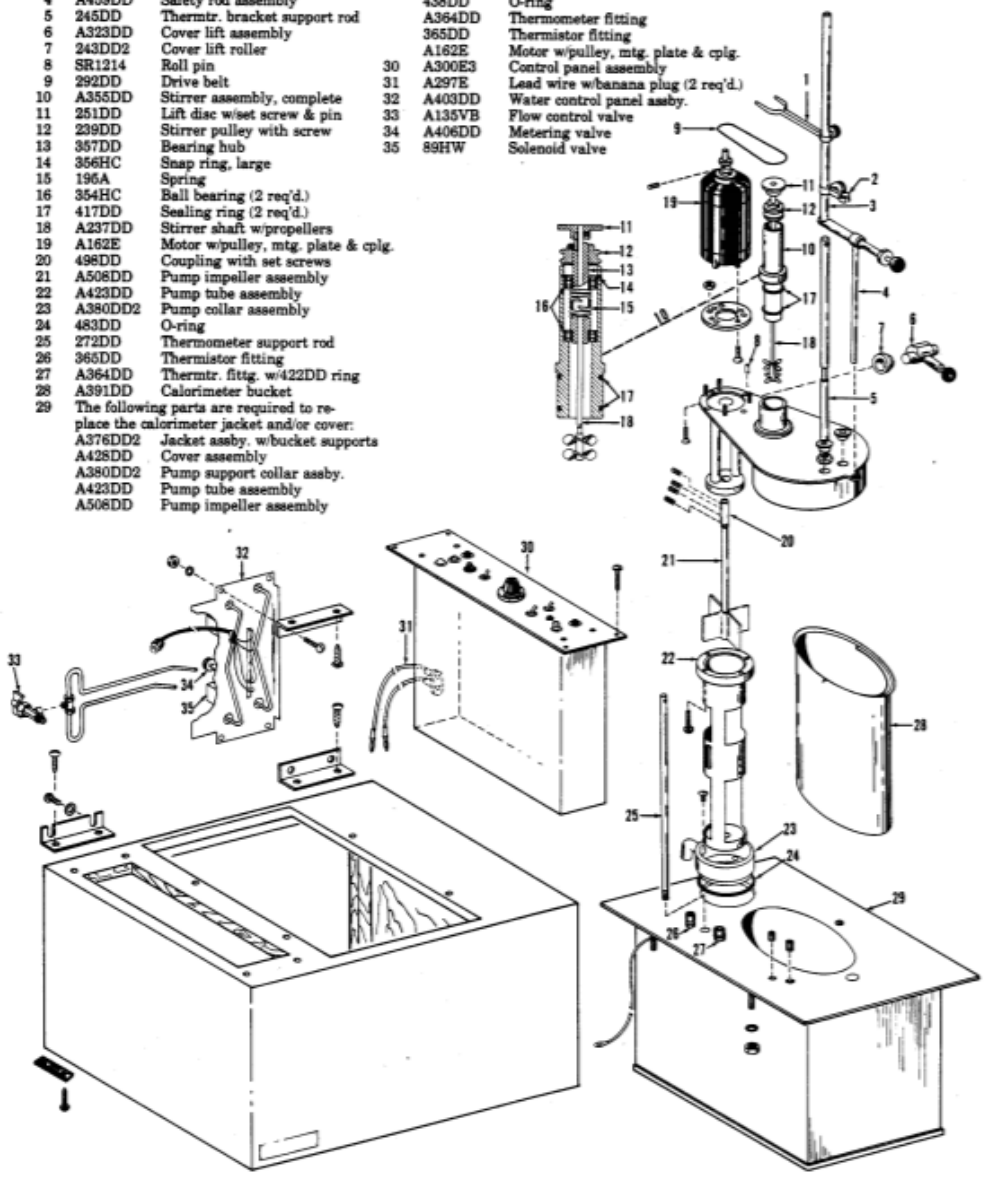

Figure F1. Diagram of 1241 Adiabatic Calorimeter Parts, by Parr Instrument Company

PARTS FOR THE 1108 OXYGEN BOMB

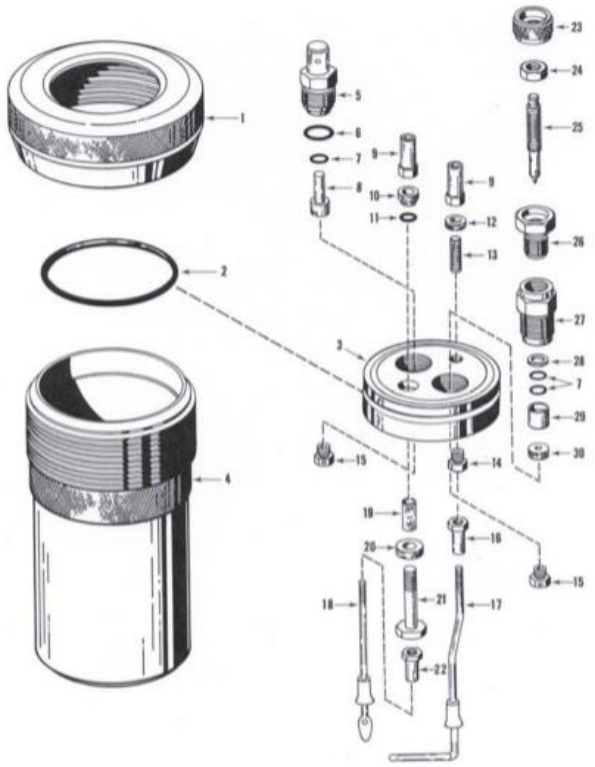

Key No.	Part No.	Description
1	103A	Screw Cap
2	230A	O-Ring,2-3/8 ID, Buna-N
3	394A12CL	Bomb Head, Bare
	394A12CL	Bomb Head, Bare, for Chlorine service
4	A101A	Bomb Cylinder, sold only with 103A screw cap as Part No. AA101A
	A101ACL	Bomb Cylinder, sold only with 103A screw cap as Part No. AA101ACL
5	395A2	Inlet Valve Body
6	415A	O-Ring, 7/16 ID, Buna-N
7	238A	O-Ring, 3/16 ID, Buna-N
8	403A	Check Valve
9	411A	Terminal Nut
10	143AC	Insulator, Delrin
11	238A	O-Ring 3/16 ID, Buna-N
12	388A	Spacer
13	SC1932SC10	Soc. Hd. Set Screw
14	278A3	Adapter Bushing
15	404A2	Deflector Nut
16	406A	Lock Nut
17	5A10	Loop Electrode with sleeve
18	4A10	Straight Electrode with sleeve
19	401A	Sleeve Insulator
20	96AC	Electrode Insulator
21	402A	Electrode Core
22	406A	Lock Nut
23	407A	Valve Knob
24	398A	Lock Nut
25	400A	Valve Needle
	A420A	Valve Needle with knob (Nos. 23,24,25)
26	397A	Compression Nut
27	396A	Outlet Valve Body
28	7VBCM	Washer, Monel
29	378A	Packing Cup
30	20VB	Valve Seat, Kel-F

Figure F2. Diagram of 1108 Oxygen Bomb Parts, by Parr Instrument Company

Appendix G. O_2 replacement during gas sampling

Assuming that the O_2 concentration reported by the Micro GC represents the fraction of the chamber pressure provided by the O_2 in the chamber, and that the total pressure of the chamber environment is 1 atm, then the target concentration of O_2 will be 0.1 atm (for the 10% O_2 treatment) or 0.2 atm (for the 20% O_2 treatment). The 0% O_2 treatment need not be considered here, as the gas replacement step for this treatment utilizes 100% N_2 gas only. In doing these calculations, there is also the assumption that the chamber headspace is constant, and the chamber temperature is known (and equal to the temperature at which the laboratory oven was set).

$PV = nRT$ (the ideal gas law) is used to calculate the moles of O_2 that should be present in the chamber for the given treatment, either 10% or 20% O_2 (labeled n_1). This step involves the desired partial pressure of O_2 (P_1 = 0.1 atm or 0.2 atm for 10% and 20% O_2 treatments, respectively), chamber headspace (V (in L), which is equal to the volume of the chambers, 0.949 L, less the volume taken up by the chip material), chamber temperature (T = 293.15 K, 313.15 K, or 333.15 K for 20°C, 40°C, and 60°C treatments, respectively), and the gas constant (R = 0.08205 atm $\cdot$ L $\cdot$ mol^{-1} $\cdot$ K^{-1}).

Equation 2 is also used to calculate the moles of O_2 that should be present in a given chamber based on the observed concentration of O_2 as reported by the Micro GC (labeled n_2). For this step, the variables used for the ideal gas law are identical to the variables above, except for P_2 (which will now reflect the partial pressure of O_2 in the chamber at the time of gas sampling). Although changes in gas composition are expected, the chamber pressure is still assumed to be consistent—findings from a study by Kuang

et al. (2008) report a maximum pressure increase of 6.9 - 8.1 kPa (0.068 - 0.079 atm) for incubation of Douglas fir woodchips at 50°C over the course of 60 days. According to Kuang et al., this relatively small change in pressure may be due to a majority of the gas (CO_2 and CO) formation being offset by the depletion of O_2 (one mole of O_2 is consumed in the generation of one mole of CO_2).

Equation 3 ($n_1 - n_2 = n$) is used to calculate the additional moles of O_2 needed to return the O_2 to the treatment level (the value for n_2 is subtracted from n_1). Once this value is obtained, it is used in Equation 2 to calculate the volume of O_2 that is needed in the syringe for gas replacement. This step also requires the pressure within the syringe (P_s = 1.0 atm), the gas constant ($R = 0.08205\ atm \cdot L \cdot mol^{-1} \cdot K^{-1}$), the volume of the syringe (0.05 L) and the temperature within the syringe, which is assumed to be equal to ambient temperature ($T_s \sim 293.15$ K). The volume of O_2 needed in the syringe is subtracted from the total syringe volume for gas replacement (0.05 L) to calculate the volume of N_2 to be added to the chamber.

Appendix H. Average gas concentrations reported by GHG analyzer by treatment

Table H1. Average CO_2 concentrations per sampling event by incubation treatment (Tx)

Date	Day	Value (ppm)	Tx
3/16/2020	3	23600	1
3/16/2020	3	11200	2
3/16/2020	3	26200	3
3/16/2020	3	25000	4
3/16/2020	3	34000	5
3/16/2020	3	33800	6
3/18/2020	5	28600	1
3/18/2020	5	17600	2
3/18/2020	5	42800	3
3/18/2020	5	40800	4
3/18/2020	5	47000	5
3/18/2020	5	44600	6
3/20/2020	7	37800	1
3/20/2020	7	17800	2
3/20/2020	7	39000	3
3/20/2020	7	43800	4
3/20/2020	7	47200	5
3/20/2020	7	44000	6
3/23/2020	10	40000	1
3/23/2020	10	19400	2
3/23/2020	10	49200	3
3/23/2020	10	49400	4
3/23/2020	10	51200	5
3/23/2020	10	57600	6
3/25/2020	12	41000	1
3/25/2020	12	21000	2
3/25/2020	12	56600	3
3/25/2020	12	54400	4
3/25/2020	12	55600	5
3/25/2020	12	68000	6
3/27/2020	14	39800	1
3/27/2020	14	24400	2
3/27/2020	14	60000	3
3/27/2020	14	64800	4
3/27/2020	14	62000	5
3/27/2020	14	78400	6
3/30/2020	17	39200	1
3/30/2020	17	24600	2
3/30/2020	17	55000	3
3/30/2020	17	58200	4
3/30/2020	17	51000	5
3/30/2020	17	76600	6
4/1/2020	19	38800	1
4/1/2020	19	25000	2
4/1/2020	19	50800	3
4/1/2020	19	55600	4
4/1/2020	19	52400	5
4/1/2020	19	78600	6
4/3/2020	21	39800	1
4/3/2020	21	30200	2
4/3/2020	21	58600	3
4/3/2020	21	54800	4
4/3/2020	21	54000	5
4/3/2020	21	81000	6
4/6/2020	24	49400	1
4/6/2020	24	47000	2
4/6/2020	24	113000	3
4/6/2020	24	20000	4
4/6/2020	24	31600	5
4/6/2020	24	57000	6
4/8/2020	26	45200	1
4/8/2020	26	38200	2
4/8/2020	26	92600	3
4/8/2020	26	49800	4

Date	Day	Value (ppm)	Tx
4/8/2020	26	37000	5
4/8/2020	26	71600	6
4/10/2020	28	65600	1
4/10/2020	28	46600	2
4/10/2020	28	123600	3
4/10/2020	28	45200	4
4/10/2020	28	63800	5
4/10/2020	28	63200	6
4/13/2020	31	50000	1
4/13/2020	31	43400	2
4/13/2020	31	84800	3
4/13/2020	31	66400	4
4/13/2020	31	59800	5
4/13/2020	31	86600	6
5/6/2020	3	10600	1
5/6/2020	3	9600	2
5/6/2020	3	23000	3
5/6/2020	3	44600	4
5/6/2020	3	24000	5
5/6/2020	3	50200	6
5/8/2020	5	15400	1
5/8/2020	5	15000	2
5/8/2020	5	48600	3
5/8/2020	5	58400	4
5/8/2020	5	67800	5
5/8/2020	5	75200	6
5/11/2020	7	19600	1
5/11/2020	7	18600	2
5/11/2020	7	57800	3
5/11/2020	7	62200	4
5/11/2020	7	94800	5
5/11/2020	7	119600	6
5/13/2020	10	21800	1
5/13/2020	10	21600	2
5/13/2020	10	58200	3
5/13/2020	10	71800	4
5/13/2020	10	118000	5
5/13/2020	10	109800	6

Date	Day	Value (ppm)	Tx
5/15/2020	12	23600	1
5/15/2020	12	20400	2
5/15/2020	12	58800	3
5/15/2020	12	69400	4
5/15/2020	12	122600	5
5/15/2020	12	128800	6
5/18/2020	14	19800	1
5/18/2020	14	26400	2
5/18/2020	14	52000	3
5/18/2020	14	66000	4
5/18/2020	14	101600	5
5/18/2020	14	150000	6
5/20/2020	17	26800	1
5/20/2020	17	30600	2
5/20/2020	17	64400	3
5/20/2020	17	78800	4
5/20/2020	17	135600	5
5/20/2020	17	126000	6
5/22/2020	19	30400	1
5/22/2020	19	36000	2
5/22/2020	19	64200	3
5/22/2020	19	83400	4
5/22/2020	19	145600	5
5/22/2020	19	88400	6
5/25/2020	21	34000	1
5/25/2020	21	36800	2
5/25/2020	21	67000	3
5/25/2020	21	94600	4
5/25/2020	21	196800	5
5/25/2020	21	140400	6
5/27/2020	24	36000	1
5/27/2020	24	39200	2
5/27/2020	24	69000	3
5/27/2020	24	93600	4
5/27/2020	24	107800	5
5/27/2020	24	115200	6
5/29/2020	26	38600	1
5/29/2020	26	43600	2

Date	Day	Value (ppm)	Tx
5/29/2020	26	69200	3
5/29/2020	26	87400	4
5/29/2020	26	133800	5
5/29/2020	26	163000	6
6/1/2020	28	44200	1
6/1/2020	28	45000	2
6/1/2020	28	81200	3
6/1/2020	28	94000	4
6/1/2020	28	179400	5
6/1/2020	28	234600	6
6/3/2020	31	43000	1
6/3/2020	31	45200	2
6/3/2020	31	77800	3
6/3/2020	31	90200	4
6/3/2020	31	154000	5
6/3/2020	31	90600	6
6/19/2020	3	7000	1
6/19/2020	3	6400	2
6/19/2020	3	9800	3
6/19/2020	3	21400	4
6/19/2020	3	15000	5
6/19/2020	3	24800	6
6/22/2020	6	10600	1
6/22/2020	6	11000	2
6/22/2020	6	22400	3
6/22/2020	6	49200	4
6/22/2020	6	31200	5
6/22/2020	6	46600	6
6/24/2020	8	13800	1
6/24/2020	8	14800	2
6/24/2020	8	32600	3
6/24/2020	8	68200	4
6/24/2020	8	44400	5
6/24/2020	8	62600	6
6/26/2020	10	16800	1
6/26/2020	10	17600	2
6/26/2020	10	38800	3
6/26/2020	10	70400	4
6/26/2020	10	52800	5
6/26/2020	10	73800	6
6/29/2020	13	20200	1
6/29/2020	13	20800	2
6/29/2020	13	55200	3
6/29/2020	13	89200	4
6/29/2020	13	74000	5
6/29/2020	13	99000	6
7/1/2020	15	22600	1
7/1/2020	15	24400	2
7/1/2020	15	68200	3
7/1/2020	15	83200	4
7/1/2020	15	89400	5
7/1/2020	15	113200	6
7/3/2020	17	24800	1
7/3/2020	17	25800	2
7/3/2020	17	67600	3
7/3/2020	17	80800	4
7/7/2020	21	20000	1
7/7/2020	21	32600	2
7/7/2020	21	87400	3
7/7/2020	21	96800	4
7/7/2020	21	111200	5
7/7/2020	21	112400	6
7/9/2020	23	30800	1
7/9/2020	23	32000	2
7/9/2020	23	90400	3
7/9/2020	23	92800	4
7/9/2020	23	113200	5
7/9/2020	23	116800	6
7/11/2020	25	36400	1
7/11/2020	25	36600	2
7/11/2020	25	99000	3
7/11/2020	25	87600	4
7/11/2020	25	87800	5
7/11/2020	25	125000	6
7/13/2020	27	41200	1
7/13/2020	27	42400	2

Date	Day	Value (ppm)	Tx
7/13/2020	27	93000	3
7/13/2020	27	100600	4
7/13/2020	27	91600	5
7/13/2020	27	109800	6
7/15/2020	29	46400	1
7/15/2020	29	45400	2
7/15/2020	29	107800	3
7/15/2020	29	94600	4
7/17/2020	31	135600	6

Date	Day	Value (ppm)	Tx
7/15/2020	29	107000	5
7/15/2020	29	126000	6
7/17/2020	31	43200	1
7/17/2020	31	44200	2
7/17/2020	31	96000	3
7/17/2020	31	95800	4
7/17/2020	31	102000	5

Table H2. Average CH_4 concentrations per sampling event by incubation treatment (Tx)

Date	Day	Value (ppm)	Tx
3/16/2020	3	2	1
3/16/2020	3	2	2
3/16/2020	3	2	3
3/16/2020	3	2	4
3/16/2020	3	3	5
3/16/2020	3	4	6
3/18/2020	5	NA	1
3/18/2020	5	2	2
3/18/2020	5	4	3
3/18/2020	5	3	4
3/18/2020	5	5	5
3/18/2020	5	6	6
3/20/2020	7	2	1
3/20/2020	7	2	2
3/20/2020	7	4	3
3/20/2020	7	4	4
3/20/2020	7	6	5
3/20/2020	7	7	6
3/23/2020	10	2	1
3/23/2020	10	2	2
3/23/2020	10	4	3
3/23/2020	10	5	4
3/23/2020	10	8	5
3/23/2020	10	9	6
3/25/2020	12	2	1
3/25/2020	12	3	2
3/25/2020	12	5	3
3/25/2020	12	7	4
3/25/2020	12	9	5
3/25/2020	12	10	6
3/27/2020	14	2	1
3/27/2020	14	2	2
3/27/2020	14	5	3
3/27/2020	14	8	4
3/27/2020	14	10	5
3/27/2020	14	10	6
3/30/2020	17	2	1
3/30/2020	17	3	2
3/30/2020	17	6	3
3/30/2020	17	9	4
3/30/2020	17	8	5
3/30/2020	17	12	6
4/1/2020	19	3	1
4/1/2020	19	3	2
4/1/2020	19	6	3
4/1/2020	19	9	4
4/1/2020	19	9	5
4/1/2020	19	13	6
4/3/2020	21	3	1
4/3/2020	21	3	2
4/3/2020	21	8	3
4/3/2020	21	8	4
4/3/2020	21	10	5
4/3/2020	21	13	6
4/6/2020	24	5	1
4/6/2020	24	4	2
4/6/2020	24	9	3
4/6/2020	24	4	4
4/6/2020	24	6	5
4/6/2020	24	7	6
4/8/2020	26	5	1
4/8/2020	26	4	2
4/8/2020	26	10	3
4/8/2020	26	10	4
4/8/2020	26	8	5
4/8/2020	26	13	6
4/10/2020	28	8	1
4/10/2020	28	5	2
4/10/2020	28	8	3
4/10/2020	28	7	4
4/10/2020	28	9	5

Date	Day	Value (ppm)	Tx
4/10/2020	28	8	6
4/13/2020	31	9	1
4/13/2020	31	6	2
4/13/2020	31	10	3
4/13/2020	31	13	4
4/13/2020	31	12	5
4/13/2020	31	15	6
5/6/2020	3	2	1
5/6/2020	3	2	2
5/6/2020	3	2	3
5/6/2020	3	2	4
5/6/2020	3	2	5
5/6/2020	3	2	6
5/8/2020	5	2	1
5/8/2020	5	2	2
5/8/2020	5	2	3
5/8/2020	5	2	4
5/8/2020	5	2	5
5/8/2020	5	2	6
5/11/2020	7	2	1
5/11/2020	7	2	2
5/11/2020	7	2	3
5/11/2020	7	2	4
5/11/2020	7	3	5
5/11/2020	7	2	6
5/13/2020	10	2	1
5/13/2020	10	2	2
5/13/2020	10	2	3
5/13/2020	10	2	4
5/13/2020	10	3	5
5/13/2020	10	3	6
5/15/2020	12	2	1
5/15/2020	12	2	2
5/15/2020	12	2	3
5/15/2020	12	2	4
5/15/2020	12	3	5
5/15/2020	12	2	6
5/18/2020	14	2	1

Date	Day	Value (ppm)	Tx
5/18/2020	14	2	2
5/18/2020	14	2	3
5/18/2020	14	2	4
5/18/2020	14	3	5
5/18/2020	14	2	6
5/20/2020	17	2	1
5/20/2020	17	2	2
5/20/2020	17	2	3
5/20/2020	17	2	4
5/20/2020	17	3	5
5/20/2020	17	3	6
5/22/2020	19	2	1
5/22/2020	19	2	2
5/22/2020	19	2	3
5/22/2020	19	2	4
5/22/2020	19	4	5
5/22/2020	19	3	6
5/25/2020	21	2	1
5/25/2020	21	2	2
5/25/2020	21	2	3
5/25/2020	21	2	4
5/25/2020	21	3	5
5/25/2020	21	3	6
5/27/2020	24	2	1
5/27/2020	24	2	2
5/27/2020	24	2	3
5/27/2020	24	2	4
5/27/2020	24	4	5
5/27/2020	24	3	6
5/29/2020	26	2	1
5/29/2020	26	2	2
5/29/2020	26	2	3
5/29/2020	26	2	4
5/29/2020	26	4	5
5/29/2020	26	3	6
6/1/2020	28	2	1
6/1/2020	28	2	2
6/1/2020	28	2	3

Date	Day	Value (ppm)	Tx
6/1/2020	28	2	4
6/1/2020	28	4	5
6/1/2020	28	3	6
6/3/2020	31	2	1
6/3/2020	31	2	2
6/3/2020	31	2	3
6/3/2020	31	2	4
6/3/2020	31	4	5
6/3/2020	31	4	6
6/19/2020	3	2	1
6/19/2020	3	2	2
6/19/2020	3	2	3
6/19/2020	3	2	4
6/19/2020	3	2	5
6/19/2020	3	2	6
6/22/2020	6	2	1
6/22/2020	6	2	2
6/22/2020	6	2	3
6/22/2020	6	2	4
6/22/2020	6	3	5
6/22/2020	6	2	6
6/24/2020	8	2	1
6/24/2020	8	2	2
6/24/2020	8	2	3
6/24/2020	8	2	4
6/24/2020	8	3	5
6/24/2020	8	2	6
6/26/2020	10	2	1
6/26/2020	10	2	2
6/26/2020	10	2	3
6/26/2020	10	2	4
6/26/2020	10	3	5
6/26/2020	10	3	6
6/29/2020	13	2	1
6/29/2020	13	2	2
6/29/2020	13	2	3
6/29/2020	13	2	4
6/29/2020	13	3	5

Date	Day	Value (ppm)	Tx
6/29/2020	13	3	6
7/1/2020	15	2	1
7/1/2020	15	2	2
7/1/2020	15	2	3
7/1/2020	15	2	4
7/1/2020	15	3	5
7/1/2020	15	3	6
7/3/2020	17	2	1
7/3/2020	17	2	2
7/3/2020	17	2	3
7/3/2020	17	2	4
7/3/2020	17	4	5
7/3/2020	17	3	6
7/7/2020	21	2	1
7/7/2020	21	2	2
7/7/2020	21	2	3
7/7/2020	21	2	4
7/7/2020	21	3	5
7/7/2020	21	3	6
7/9/2020	23	2	1
7/9/2020	23	2	2
7/9/2020	23	2	3
7/9/2020	23	2	4
7/9/2020	23	3	5
7/9/2020	23	3	6
7/11/2020	25	2	1
7/11/2020	25	2	2
7/11/2020	25	2	3
7/11/2020	25	2	4
7/11/2020	25	3	5
7/11/2020	25	3	6
7/13/2020	27	2	1
7/13/2020	27	2	2
7/13/2020	27	2	3
7/13/2020	27	2	4
7/13/2020	27	4	5
7/13/2020	27	3	6
7/15/2020	29	2	1

Date	Day	Value (ppm)	Tx
7/15/2020	29	2	2
7/15/2020	29	2	3
7/15/2020	29	2	4
7/15/2020	29	3	5
7/15/2020	29	3	6
7/17/2020	31	2	1

Date	Day	Value (ppm)	Tx
7/17/2020	31	2	2
7/17/2020	31	2	3
7/17/2020	31	2	4
7/17/2020	31	4	5
7/17/2020	31	4	6

Table H3. Average N_2O concentrations per sampling event by incubation treatment (Tx)

Date	Day	Value (ppm)	Tx
3/16/2020	3	0.5	1
3/16/2020	3	0.5	2
3/16/2020	3	0.5	3
3/16/2020	3	0.5	4
3/16/2020	3	0.5	5
3/16/2020	3	2	6
3/18/2020	5	0.5	1
3/18/2020	5	1	2
3/18/2020	5	1.5	3
3/18/2020	5	0.5	4
3/18/2020	5	1	5
3/18/2020	5	0.5	6
3/20/2020	7	0.5	1
3/20/2020	7	0.5	2
3/20/2020	7	1.5	3
3/20/2020	7	1	4
3/20/2020	7	0.5	5
3/20/2020	7	0.5	6
3/23/2020	10	0.5	1
3/23/2020	10	0.5	2
3/23/2020	10	0.5	3
3/23/2020	10	1.5	4
3/23/2020	10	0.5	5
3/23/2020	10	1	6
3/25/2020	12	0.5	1
3/25/2020	12	2	2
3/25/2020	12	0.5	3
3/25/2020	12	0.5	4
3/25/2020	12	2	5
3/25/2020	12	0.5	6
3/27/2020	14	0.5	1
3/27/2020	14	0.5	2
3/27/2020	14	1	3
3/27/2020	14	6	4
3/27/2020	14	1.5	5
3/27/2020	14	0.5	6
3/30/2020	17	0.5	1
3/30/2020	17	0.5	2
3/30/2020	17	1.5	3
3/30/2020	17	0.5	4
3/30/2020	17	1	5
3/30/2020	17	0.5	6
4/1/2020	19	1	1
4/1/2020	19	0.5	2
4/1/2020	19	0.5	3
4/1/2020	19	5	4
4/1/2020	19	1	5
4/1/2020	19	1.5	6
4/3/2020	21	0.5	1
4/3/2020	21	0.5	2
4/3/2020	21	1	3
4/3/2020	21	1	4
4/3/2020	21	1	5
4/3/2020	21	1	6
4/6/2020	24	2.5	1
4/6/2020	24	1	2
4/6/2020	24	1	3
4/6/2020	24	0.5	4
4/6/2020	24	0.5	5
4/6/2020	24	1	6
4/8/2020	26	0.5	1
4/8/2020	26	0.5	2
4/8/2020	26	0.5	3
4/8/2020	26	1	4
4/8/2020	26	1	5
4/8/2020	26	0.5	6
4/10/2020	28	1	1
4/10/2020	28	2	2
4/10/2020	28	1	3
4/10/2020	28	1.5	4

Date	Day	Value (ppm)	Tx
4/10/2020	28	0.5	5
4/10/2020	28	0.5	6
4/13/2020	31	1	1
4/13/2020	31	0.5	2
4/13/2020	31	0.5	3
4/13/2020	31	0.5	4
4/13/2020	31	0.5	5
4/13/2020	31	1	6
5/6/2020	3	0.5	1
5/6/2020	3	0.5	2
5/6/2020	3	0.5	3
5/6/2020	3	0.5	4
5/6/2020	3	0.5	5
5/6/2020	3	0.5	6
5/8/2020	5	0.5	1
5/8/2020	5	0.5	2
5/8/2020	5	0.5	3
5/8/2020	5	0.5	4
5/8/2020	5	0.5	5
5/8/2020	5	0.5	6
5/11/2020	7	0.5	1
5/11/2020	7	0.5	2
5/11/2020	7	0.5	3
5/11/2020	7	0.5	4
5/11/2020	7	0.5	5
5/11/2020	7	0.5	6
5/13/2020	10	0.5	1
5/13/2020	10	0.5	2
5/13/2020	10	0.5	3
5/13/2020	10	0.5	4
5/13/2020	10	0.5	5
5/13/2020	10	0.5	6
5/15/2020	12	0.5	1
5/15/2020	12	0.5	2
5/15/2020	12	0.5	3
5/15/2020	12	0.5	4
5/15/2020	12	0.5	5
5/15/2020	12	0.5	6

Date	Day	Value (ppm)	Tx
5/18/2020	14	0.5	1
5/18/2020	14	1	2
5/18/2020	14	0.5	3
5/18/2020	14	0.5	4
5/18/2020	14	0.5	5
5/18/2020	14	0.5	6
5/20/2020	17	1.5	1
5/20/2020	17	0.5	2
5/20/2020	17	0.5	3
5/20/2020	17	0.5	4
5/20/2020	17	0.5	5
5/20/2020	17	0.5	6
5/22/2020	19	0.5	1
5/22/2020	19	0.5	2
5/22/2020	19	0.5	3
5/22/2020	19	0.5	4
5/22/2020	19	1.5	5
5/22/2020	19	0.5	6
5/25/2020	21	0.5	1
5/25/2020	21	1	2
5/25/2020	21	0.5	3
5/25/2020	21	0.5	4
5/25/2020	21	0.5	5
5/25/2020	21	1.5	6
5/27/2020	24	1	1
5/27/2020	24	1	2
5/27/2020	24	0.5	3
5/27/2020	24	0.5	4
5/27/2020	24	0.5	5
5/27/2020	24	0.5	6
5/29/2020	26	0.5	1
5/29/2020	26	0.5	2
5/29/2020	26	0.5	3
5/29/2020	26	0.5	4
5/29/2020	26	0.5	5
5/29/2020	26	1	6
6/1/2020	28	0.5	1
6/1/2020	28	2.5	2

Date	Day	Value (ppm)	Tx
6/1/2020	28	0.5	3
6/1/2020	28	0.5	4
6/1/2020	28	0.5	5
6/1/2020	28	0.5	6
6/3/2020	31	0.5	1
6/3/2020	31	0.5	2
6/3/2020	31	0.5	3
6/3/2020	31	0.5	4
6/3/2020	31	0.5	5
6/3/2020	31	0.5	6
6/19/2020	3	0.5	1
6/19/2020	3	0.5	2
6/19/2020	3	0.5	3
6/19/2020	3	0.5	4
6/19/2020	3	0.5	5
6/19/2020	3	0.5	6
6/22/2020	6	0.5	1
6/22/2020	6	0.5	2
6/22/2020	6	0.5	3
6/22/2020	6	0.5	4
6/22/2020	6	0.5	5
6/22/2020	6	0.5	6
6/24/2020	8	0.5	1
6/24/2020	8	0.5	2
6/24/2020	8	0.5	3
6/24/2020	8	0.5	4
6/24/2020	8	0.5	5
6/24/2020	8	0.5	6
6/26/2020	10	0.5	1
6/26/2020	10	0.5	2
6/26/2020	10	0.5	3
6/26/2020	10	0.5	4
6/26/2020	10	0.5	5
6/26/2020	10	0.5	6
6/29/2020	13	0.5	1
6/29/2020	13	0.5	2
6/29/2020	13	0.5	3
6/29/2020	13	0.5	4

Date	Day	Value (ppm)	Tx
6/29/2020	13	0.5	5
6/29/2020	13	0.5	6
7/1/2020	15	0.5	1
7/1/2020	15	0.5	2
7/1/2020	15	0.5	3
7/1/2020	15	0.5	4
7/1/2020	15	0.5	5
7/1/2020	15	0.5	6
7/3/2020	17	0.5	1
7/3/2020	17	0.5	2
7/3/2020	17	0.5	3
7/3/2020	17	0.5	4
7/3/2020	17	0.5	5
7/3/2020	17	0.5	6
7/7/2020	21	0.5	1
7/7/2020	21	0.5	2
7/7/2020	21	0.5	3
7/7/2020	21	0.5	4
7/7/2020	21	0.5	5
7/7/2020	21	0.5	6
7/9/2020	23	0.5	1
7/9/2020	23	0.5	2
7/9/2020	23	0.5	3
7/9/2020	23	0.5	4
7/9/2020	23	0.5	5
7/9/2020	23	0.5	6
7/11/2020	25	0.5	1
7/11/2020	25	0.5	2
7/11/2020	25	0.5	3
7/11/2020	25	0.5	4
7/11/2020	25	0.5	5
7/11/2020	25	0.5	6
7/13/2020	27	0.5	1
7/13/2020	27	0.5	2
7/13/2020	27	0.5	3
7/13/2020	27	0.5	4
7/13/2020	27	0.5	5
7/13/2020	27	0.5	6

Date	Day	Value (ppm)	Tx
7/15/2020	29	0.5	1
7/15/2020	29	0.5	2
7/15/2020	29	0.5	3
7/15/2020	29	0.5	4
7/15/2020	29	0.5	5
7/15/2020	29	0.5	6

Date	Day	Value (ppm)	Tx
7/17/2020	31	0.5	1
7/17/2020	31	1	2
7/17/2020	31	0.5	3
7/17/2020	31	0.5	4
7/17/2020	31	0.5	5
7/17/2020	31	0.5	6

Appendix I. Energy content testing results via bomb calorimetry

Table I1. Results of energy content testing for incubated and unincubated chip samples at 20°C, n = 3.

Fuel material	Fuel type	Average energy content (MJ/kg)	SE
Redwood chips	Unincubated, 50% moisture	19.1	0.223
Redwood chips	Incubated, 20°C, 50% moisture, 0% O2	20.1	0.115
Redwood chips	Incubated, 20°C, 50% moisture, 20% O2	19.6	0.198

Appendix J. Cumulative gas emissions tables

Table J1. Cumulative gas emissions of CO_2 (g) by chamber

Chamber	Oxygen Concentration	Moisture	60°C	40°C	20°C
1	0%	50%	62.28	61.8	60.65
2	0%	50%	125.45	78.42	56.17
3	0%	50%	94.55	55.82	62.19
4	0%	70%	40.27	56.41	60.58
5	0%	70%	60.4	70.02	62.09
6	0%	70%	96.72	56.35	57.69
7	10%	50%	124.99	83.24	135.72
8	10%	50%	185.02	121.09	151.93
9	10%	50%	155.99	118.17	119.53
10	10%	70%	188.32	125.01	143.42
11	10%	70%	174.98	136.03	148.17
12	10%	70%	188.94	137.56	157.34
13	20%	50%	181	129.31	141.07
14	20%	50%	196.47	173.75	145.49
15	20%	50%	176.42	148.2	144.69
16	20%	70%	174.22	151.47	146.31
17	20%	70%	191.56	150.33	152.74
18	20%	70%	190.77	160.95	163.6

Table J2. Cumulative gas emissions of CH_4 (g) by chamber

Chamber	Oxygen Concentration	Moisture	60°C	40°C	20°C
1	0%	50%	1.1E-02	3.0E-03	3.0E-03
2	0%	50%	1.1E-02	4.0E-03	3.0E-03
3	0%	50%	1.5E-02	3.0E-03	3.0E-03
4	0%	70%	7.0E-03	3.0E-03	3.0E-03
5	0%	70%	8.0E-03	3.0E-03	3.0E-03
6	0%	70%	8.0E-03	4.0E-03	3.0E-03
7	10%	50%	1.5E-02	3.0E-03	4.0E-03
8	10%	50%	1.3E-02	4.0E-03	4.0E-03
9	10%	50%	1.4E-02	4.0E-03	4.0E-03
10	10%	70%	1.4E-02	4.0E-03	4.0E-03
11	10%	70%	1.4E-02	4.0E-03	3.0E-03
12	10%	70%	1.5E-02	4.0E-03	4.0E-03
13	20%	50%	1.4E-02	4.0E-03	3.0E-03
14	20%	50%	1.7E-02	4.0E-03	4.0E-03
15	20%	50%	1.4E-02	4.0E-03	4.0E-03
16	20%	70%	1.4E-02	4.0E-03	4.0E-03
17	20%	70%	1.6E-02	4.0E-03	4.0E-03
18	20%	70%	1.6E-02	4.0E-03	4.0E-03

Table J3. Cumulative gas emissions of N_2O (g) by chamber

Chamber	Oxygen Concentration	Moisture	60°C	40°C	20°C
1	0%	50%	1.0E-03	7.0E-04	5.0E-04
2	0%	50%	5.2E-03	8.0E-04	5.0E-04
3	0%	50%	1.9E-03	7.0E-04	5.0E-04
4	0%	70%	3.4E-03	6.0E-04	5.0E-04
5	0%	70%	4.7E-03	7.0E-04	5.0E-04
6	0%	70%	6.1E-03	1.4E-03	5.0E-04
7	10%	50%	5.2E-03	8.0E-04	7.0E-04
8	10%	50%	1.7E-02	2.0E-03	7.0E-04
9	10%	50%	3.3E-03	4.1E-03	1.1E-03
10	10%	70%	1.7E-02	2.2E-03	7.0E-04
11	10%	70%	1.7E-02	2.1E-03	7.0E-04
12	10%	70%	1.8E-02	2.1E-03	7.0E-04
13	20%	50%	1.7E-02	2.1E-03	7.0E-04
14	20%	50%	1.7E-02	2.2E-03	7.0E-04
15	20%	50%	1.7E-02	2.1E-03	7.0E-04
16	20%	70%	1.7E-02	2.1E-03	7.0E-04
17	20%	70%	1.7E-02	2.4E-03	7.0E-04
18	20%	70%	1.7E-02	2.1E-03	8.0E-04

Table J4. Cumulative CO_2e emissions (g, using a global warming potential of 28 for CH_4 and 265 for N_2O)

Chamber	Oxygen Concentration	Moisture	60°C	40°C	20°C
1	0%	50%	6.3E+01	6.2E+01	6.1E+01
2	0%	50%	1.3E+02	7.9E+01	5.6E+01
3	0%	50%	9.6E+01	5.6E+01	6.2E+01
4	0%	70%	4.1E+01	5.7E+01	6.1E+01
5	0%	70%	6.2E+01	7.0E+01	6.2E+01
6	0%	70%	9.9E+01	5.7E+01	5.8E+01
7	10%	50%	1.3E+02	8.4E+01	1.4E+02
8	10%	50%	1.9E+02	1.2E+02	1.5E+02
9	10%	50%	1.6E+02	1.2E+02	1.2E+02
10	10%	70%	1.9E+02	1.3E+02	1.4E+02
11	10%	70%	1.8E+02	1.4E+02	1.5E+02
12	10%	70%	1.9E+02	1.4E+02	1.6E+02
13	20%	50%	1.9E+02	1.3E+02	1.4E+02
14	20%	50%	2.0E+02	1.7E+02	1.5E+02
15	20%	50%	1.8E+02	1.5E+02	1.5E+02
16	20%	70%	1.8E+02	1.5E+02	1.5E+02
17	20%	70%	2.0E+02	1.5E+02	1.5E+02
18	20%	70%	2.0E+02	1.6E+02	1.6E+02

Appendix K. Q-Q plots of multiple linear regression analyses

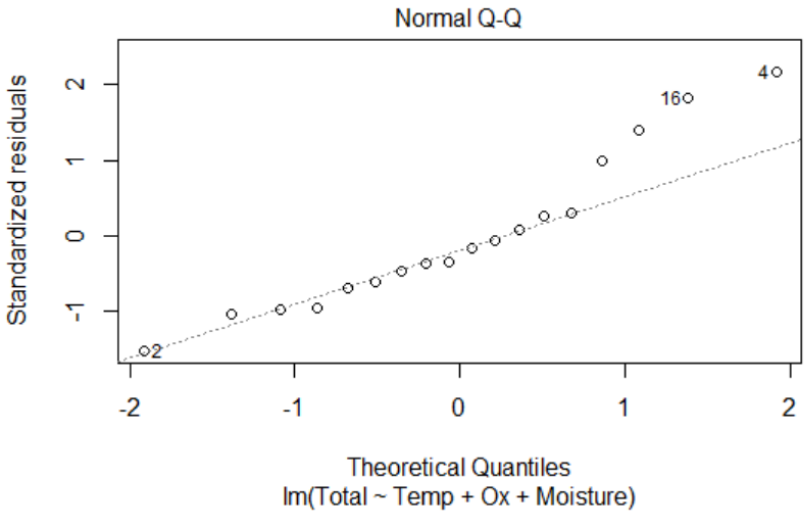

Figure K1. Q-Q plot of multiple linear regression analysis on CO_2 as a function of temperature, oxygen, and moisture

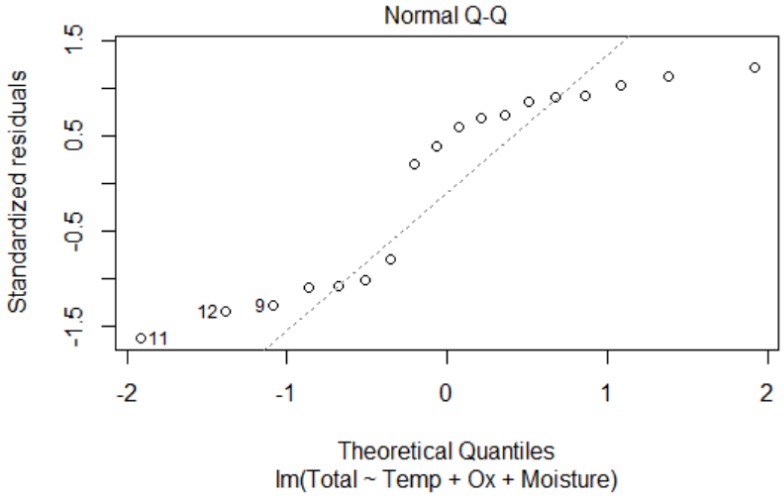

Figure K2. Q-Q plot of multiple linear regression analysis on CH_4 as a function of temperature, oxygen, and moisture

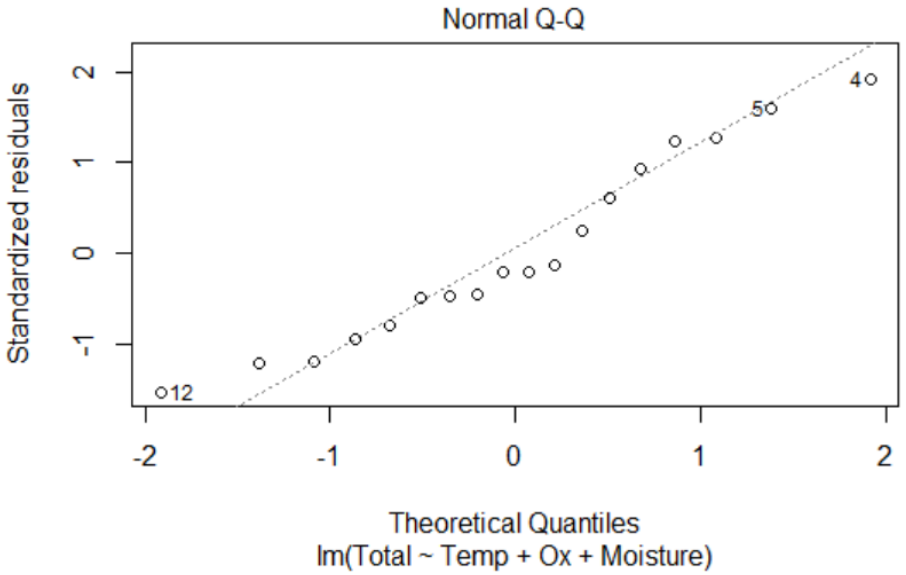

Figure K3. Q-Q plot of multiple linear regression analysis on N_2O as a function of temperature, oxygen, and moisture

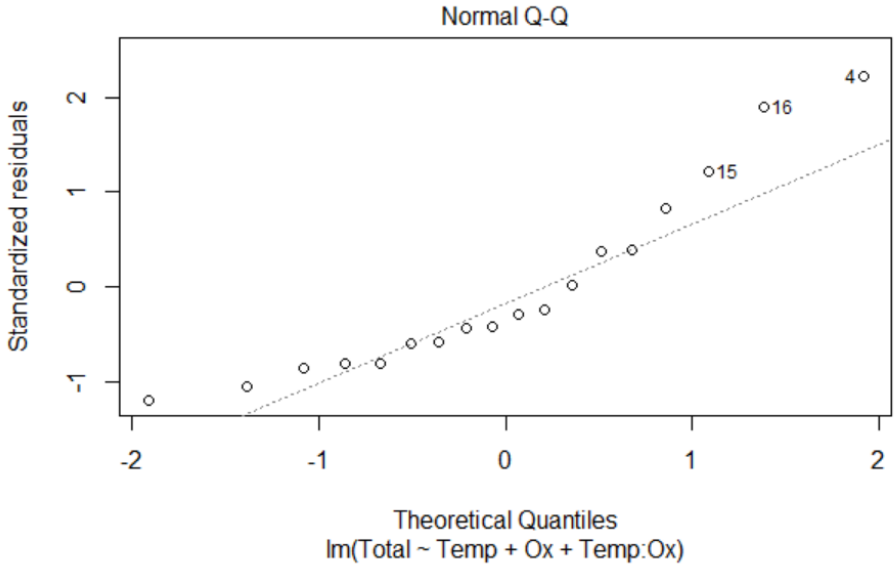

Figure K4. Q-Q plot of multiple linear regression analysis on CO_2 as a function of temperature and oxygen

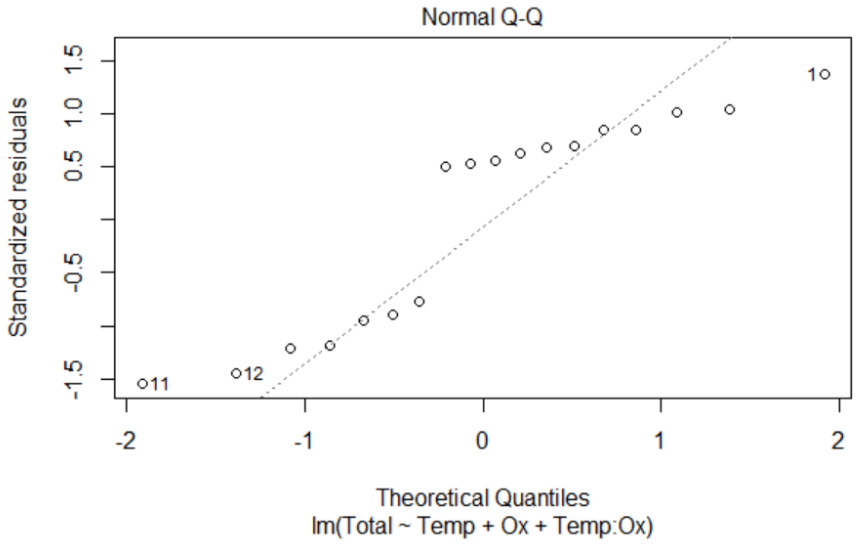

Figure K5. Q-Q plot of multiple linear regression analysis on CH_4 as a function of temperature and oxygen

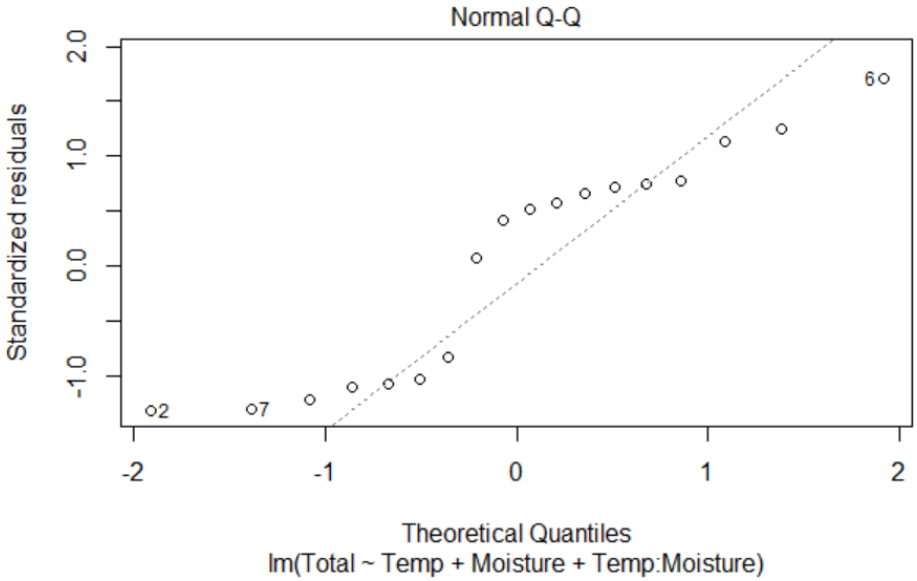

Figure K6. Q-Q plot of multiple linear regression analysis on CH_4 as a function of temperature and moisture

Appendix L. O_2 concentration over time

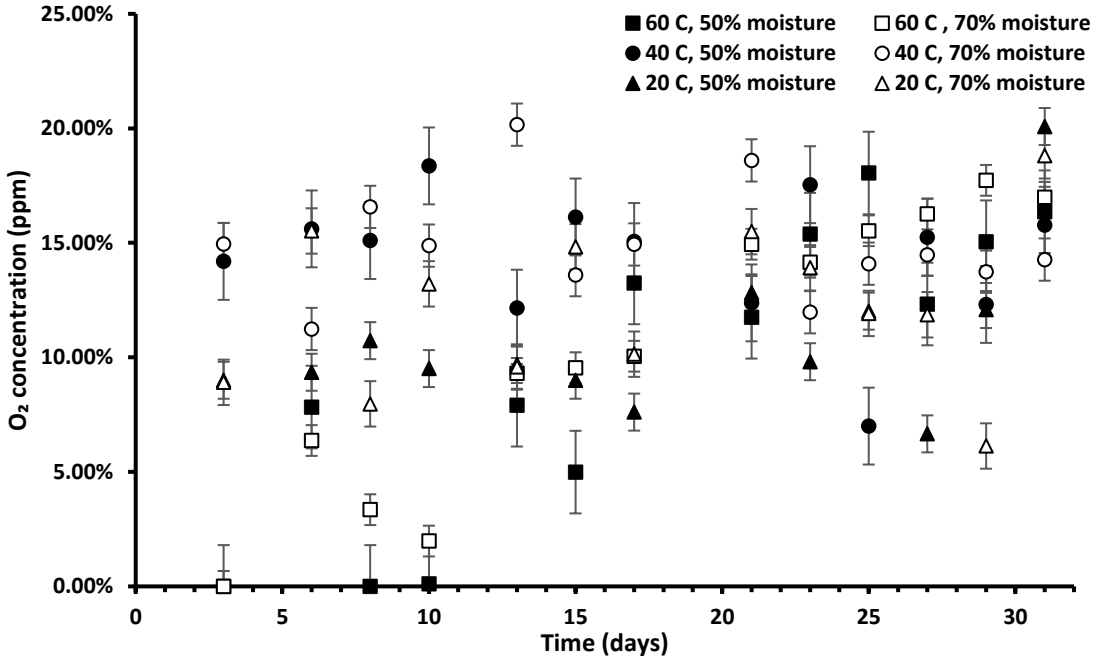

Figure L1. O_2 concentration of treatments assigned 0% O_2 over incubation period

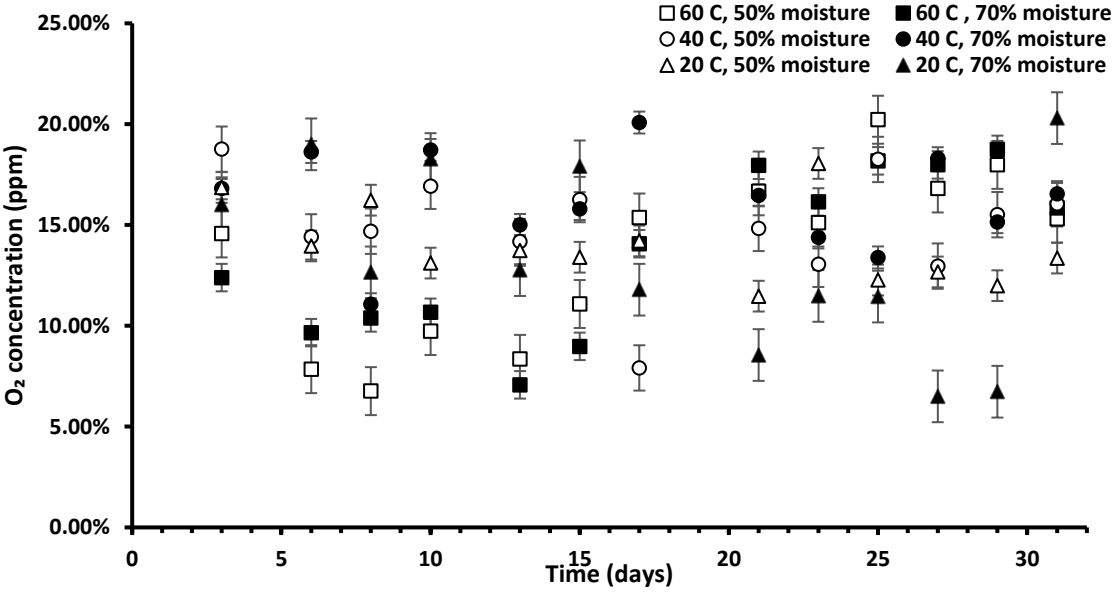

Figure L2. O_2 concentration of treatments assigned 10% O_2 over incubation period

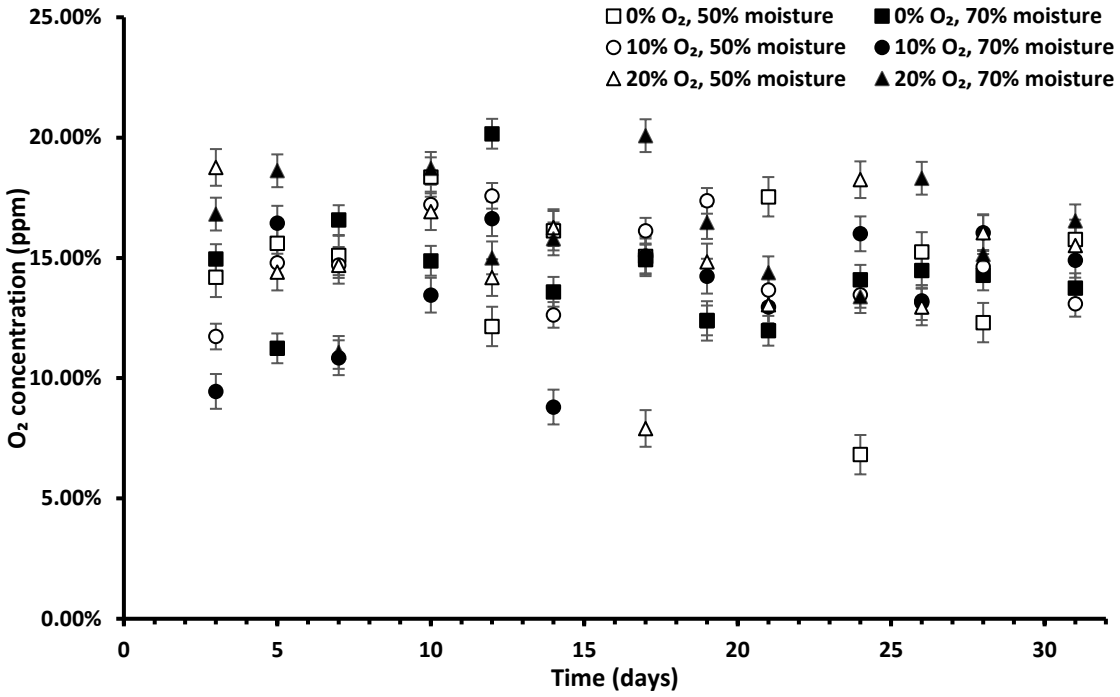

Figure L3. O_2 concentration of treatments assigned 20% O_2 over incubation period